Two structural components in CNGA3 support regulation of cone CNG channels by phosphoinositides

Gucan Dai,[1,2] Changhong Peng,[1] Chunming Liu,[1,2] and Michael D. Varnum[1,2,3]

[1]Department of Integrative Physiology and Neuroscience, [2]Program in Neuroscience, and [3]Center for Integrated Biotechnology, Washington State University, Pullman, WA 99164

Cyclic nucleotide-gated (CNG) channels in retinal photoreceptors play a crucial role in vertebrate phototransduction. The ligand sensitivity of photoreceptor CNG channels is adjusted during adaptation and in response to paracrine signals, but the mechanisms involved in channel regulation are only partly understood. Heteromeric cone CNGA3 (A3) + CNGB3 (B3) channels are inhibited by membrane phosphoinositides (PIP_n), including phosphatidylinositol 3,4,5-triphosphate (PIP_3) and phosphatidylinositol 4,5-bisphosphate (PIP_2), demonstrating a decrease in apparent affinity for cyclic guanosine monophosphate (cGMP).

Unlike homomeric A1 or A2 channels, A3-only channels paradoxically did not show a decrease in apparent affinity for cGMP after PIP_n application. However, PIP_n induced an ∼2.5-fold increase in cAMP efficacy for A3 channels. The PIP_n-dependent change in cAMP efficacy was abolished by mutations in the C-terminal region (R643Q/R646Q) or by truncation distal to the cyclic nucleotide-binding domain (613X). In addition, A3-613X unmasked a threefold decrease in apparent cGMP affinity with PIP_n application to homomeric channels, and this effect was dependent on conserved arginines within the N-terminal region of A3. Together, these results indicate that regulation of A3 subunits by phosphoinositides exhibits two separable components, which depend on structural elements within the N- and C-terminal regions, respectively. Furthermore, both N and C regulatory modules in A3 supported PIP_n regulation of heteromeric A3+B3 channels. B3 subunits were not sufficient to confer PIP_n sensitivity to heteromeric channels formed with PIP_n-insensitive A subunits. Finally, channels formed by mixtures of PIP_n-insensitive A3 subunits, having complementary mutations in N- and/or C-terminal regions, restored PIP_n regulation, implying that intersubunit N–C interactions help control the phosphoinositide sensitivity of cone CNG channels.

The Journal of General Physiology

INTRODUCTION

CNG channels are known for their essential contribution to sensory transduction in photoreceptors and olfactory sensory neurons, and for their expression in other diverse cell types where their physiological actions are less well defined (Kaupp and Seifert, 2002; Burns and Arshavsky, 2005). Six genes in mammals encode pore-forming CNG channel subunits: CNGA1 (A1), A2, A3, A4, B1, and B3. Each subunit presents cytoplasmic N- and C-terminal regions, a conserved pore domain, a vestigial voltage-sensor domain homologous to that of related voltage-gated channels, and an intracellular cyclic nucleotide-binding (CNBD) domain. Ligand binding (cyclic guanosine monophosphate [cGMP] or cAMP) to one or more of these intracellular sites is coupled to opening of the channel pore. Native CNG channels are formed by the assembly of some combination of these subunits in a tetrameric complex, generating channels with properties optimized for the role they play in specific cell types (Kaupp and Seifert, 2002; Craven and Zagotta, 2006). The principal rod photoreceptor, olfactory receptor, and cone photoreceptor CNG channels are composed of 3A1:B1 (Weitz et al., 2002; Zheng et al., 2002; Zhong et al., 2002), 2A2:A4:B1b (Zheng and Zagotta, 2004), or 2A3:2B3 subunits (Peng et al., 2004; but see also Ding et al., 2012), respectively. The B1, A4, and B3 subunits alone cannot form functional homomeric channels, but commonly modify ligand sensitivity and channel regulation properties in heteromeric channels.

CNG channel activity can be modulated by diverse intracellular messengers, including calcium feedback via calmodulin (CaM) or related calcium sensor proteins (Hsu and Molday, 1993; Liu et al., 1994; Gordon et al., 1995b; Sagoo and Lagnado, 1996; Trudeau and Zagotta, 2003; Bradley et al., 2004; Rebrik and Korenbrot, 2004; Rebrik et al., 2012), serine/threonine and tyrosine-phosphorylation events (Gordon et al., 1992; Molokanova

Correspondence to Michael D. Varnum: varnum@wsu.edu

Chunming Liu's present address is College of Optometry, Western University of Health Sciences, Pomona, CA 91766.

Abbreviations used in this paper: CaM, calmodulin; cGMP, cyclic guanosine monophosphate; CLZ, C-terminal leucine zipper; CNBD, cyclic nucleotide-binding domain; cRNA, complimentary RNA; cyto D, cytochalasin D; HNG, hyperpolarization-activated CNG; PIP_2, phosphatidylinositol (4,5)-biphosphate; PIP_3, phosphatidylinositol (3,4,5)-trisphosphate.

The Rockefeller University Press $30.00
J. Gen. Physiol. Vol. 141 No. 4 413–430
www.jgp.org/cgi/doi/10.1085/jgp.201210944

et al., 1999; Chae et al., 2007), and lipid signaling molecules such as diacylglycerol and phosphoinositides (Gordon et al., 1995a; Womack et al., 2000; Crary et al., 2000; Zhainazarov et al., 2004; Brady et al., 2006; Bright et al., 2007). These adjustments of CNG channel ligand sensitivity are thought to be integral to several important physiological processes, including but not limited to olfactory receptor and photoreceptor adaptation (Kurahashi and Menini, 1997; Fain et al., 2001), and paracrine and circadian control of photoreceptor sensitivity (Ko et al., 2003, 2004; Chen et al., 2007). In general, the control of ion channel activity by phosphoinositides has emerged recently as a nearly universal feature of many different classes of channels. For most channels, activity is supported or potentiated by phosphoinositides, particularly phosphatidylinositol (4,5)-biphosphate (PIP_2; Suh and Hille, 2008). Phosphoinositides such as PIP_2 or phosphatidylinositol (3,4,5)-trisphosphate (PIP_3) have been shown to inhibit the activity of native and recombinant rod (Womack et al., 2000), cone (Womack et al., 2000; Bright et al., 2007), and olfactory (Spehr et al., 2002; Brady et al., 2006) CNG channels. For example, the ligand sensitivity of A3+B3 channels is sensitive to manipulations of endogenous phosphoinositides using chemical or pharmacological tools, as well as direct application of phosphoinositides to inside-out patches (Bright et al., 2007). With the exception of the olfactory channel (Brady et al., 2006), little is known about the molecular mechanisms underlying regulation of CNG channels by phosphoinositides. For olfactory CNG channels, the N-terminal region of CNGA2 subunits is necessary for regulation by PIP_3, most likely by providing a phosphoinositide-binding site. Moreover, PIP_3 binding to A4 and B1b subunits attenuates CaM regulation of olfactory CNG channels (Brady et al., 2006), which suggests a functional interaction between different regulatory pathways. For photoreceptor CNG channels, the specific subunits, structural elements, and interactions that mediate phosphoinositide control have remained unanswered questions.

In this paper, we have investigated mechanisms supporting regulation of cone photoreceptor CNG channels by phosphoinositides using heterologous expression of channel subunits, electrophysiology, and molecular manipulations. Here we have identified features within CNGA3 subunits that are necessary for inhibition by PIP_2 or PIP_3. Our results suggest that regulation is mediated by two structural components, located within the cytoplasmic N- and C-terminal domains of CNGA3, respectively. These two separable components have divergent effects on gating of homomeric channels, but both contribute to the PIP_n-induced change in cGMP apparent affinity for heteromeric CNGA3+CNGB3 channels. In addition, we find that complementary combinations of PIP_n-insensitive subunits can reconstitute regulation, which is consistent with intersubunit coupling between these N- and C-terminal regions.

MATERIALS AND METHODS

DNA and mutagenesis

Human CNGB3 was cloned as described previously (Peng et al., 2003a). Human CNGA3 was a gift of K.-W. Yau (Johns Hopkins University, Baltimore, MD). Bovine CNGA1, rat CNGA2, and human CNGB1 were generously provided by W. Zagotta (University of Washington, Seattle, WA). Subunit cDNAs were subcloned into pGEMHE, where they are flanked by the *Xenopus laevis* β-globin gene 5′ and 3′ untranslated regions (UTRs), for heterologous expression in *X. laevis* oocytes. Point mutations were generated by overlapping PCR (cassette) mutagenesis. All mutations were confirmed by fluorescence-based DNA sequencing. Concatenated cDNA constructs were generated as described previously, where the stop codon for the leading subunit and the start codon for the trailing subunit were replaced by a short linker sequence (IAGGGGGRARLPA), combining the coding sequences for the two subunits in a single open reading frame (Peng et al., 2004). Previous studies using A3//A3 dimers (Peng et al., 2004) suggest that the linker has only a slight effect on the activation properties of the channels. The cDNA and transcribed complimentary RNA (cRNA) of the tandem–dimer constructs were checked for recombination by agarose gel electrophoresis.

PIP_3-binding assays

Recombinant GST fusion protein expression in bacteria and lipid interaction assays were performed as described previously (Peng et al., 2003a; Brady et al., 2006). After purification, soluble GST fusion proteins were isolated after centrifugation at 20,000 *g* and 4°C for 30 min to remove insoluble material. GST fusion proteins were then used for in vitro PIP_3-binding assays in buffer containing 10 mM Hepes, pH 7.4, 50 mM NaCl, 2 mM EDTA, 0.25% vol/vol Triton X-100, and 0.25% vol/vol Nonidet P-40. PIP_3-agarose beads were from Echelon Biosciences. In brief, 40 µl of a 50% slurry of PIP_3 or control agarose beads and purified protein (2 µg/ml) was incubated in 0.5 ml of binding buffer for 2 h at 4°C with rocking. Beads were gently pelleted and washed five times with excess binding buffer; PIP_3-interacting proteins were eluted with 1× NuPAGE sample buffer (Invitrogen). Protein samples then were separated under reducing conditions in 4–12% Bis-Tris gels and blotted onto nitrocellulose by using the NuPAGE transfer buffer system (Invitrogen). Blotted proteins were detected overnight by using B-14 anti-GST monoclonal antibody (Santa Cruz Biotechnology, Inc.) at a dilution of 1:2,000 in 1% milk, 500 mM NaCl, 20 mM Tris-HCl (pH 7.5), and 0.05% Tween 20. Anti-actin antibody (EMD Millipore) was used to ensure the same amount of input protein was used. Horseradish peroxide–conjugated anti–mouse IgG secondary antibodies were used subsequently for 1 h. Chemiluminescent detection was performed using the Super-Signal West Dura Extended Duration substrate chemiluminescence detection kit (Thermo Fisher Scientific).

Electrophysiology

For expression in *X. laevis* oocytes, channel subunit cDNAs were linearized by digestion with NheI or SphI, and cRNA was synthesized in vitro using an upstream T-7 promoter (mMessage mMachine; Ambion). Stage IV oocytes were isolated as described previously (Varnum et al., 1995). The animal-use protocols were consistent with the recommendations of the American Veterinary Medical Association and were approved by the Institutional Animal Care and Use Committee (IACUC) of Washington State University. Approximately 20 ng of channel RNA was microinjected per oocyte; to efficiently generate heteromeric channels, an excess of B subunit RNA relative to A subunit RNA was injected (Peng et al., 2004). 2–7 d after microinjection of in vitro transcribed cRNA into oocytes, patch-clamp experiments were performed using an Axopatch 200B amplifier (Molecular Devices)

in the inside-out configuration. Recordings were made at 20–22°C. Initial pipette resistances were 0.30–0.80 Mohm. Intracellular (bath) and extracellular (pipette) solutions contained 130 mM NaCl, 0.2 mM EDTA, and 3 mM Hepes, pH 7.2. Cyclic nucleotides were added to intracellular solution as needed. Intracellular solutions were changed using an RSC-160 rapid solution changer (Molecular Kinetics). For Ca^{2+}-CaM experiments, 250 nM CaM was used in intracellular solution containing 130 mM NaCl, 3 mM Hepes, pH 7.2, 3.6 mM $CaCl_2$, and 10 mM hydroxyethyl ethylenediaminetriacetic acid (HEDTA), for a final [Ca^{2+}] of 2 µM. 500 µM niflumic acid was added to the pipette solution for Ca^{2+}-CaM experiments. PIP_n solutions were prepared with FVPP (a phosphatase inhibitor cocktail; Huang et al., 1998) containing 5 mM sodium fluoride, 0.1 mM sodium orthovanadate, and 10 mM sodium pyrophosphate, as described previously (Bright et al., 2007); FVPP seems to stabilize PIP_n effects and slow reversal during washout (Bright et al., 2007). PIP_3 and PIP_2 analogues were PIP_3, dipalmitoyl, sodium salt and PIP_2, dipalmitoyl, sodium salt (Matreya LLC). Natural brain PIP_2 was from Avanti Polar Lipids, Inc. Poly-lysine and cytochalasin D (cyto D) were obtained from Sigma-Aldrich.

Data analysis

Data were acquired and analyzed using Pulse (HEKA), Igor (WaveMetrics), and SigmaPlot/SigmaStat (Systat Software). Currents in the absence of cyclic nucleotide were subtracted. For channel activation by cyclic nucleotides, dose–response data were fitted with the Hill equation, $I/I_{max} = [cNMP]^h/(K_{1/2}{}^h + [cNMP]^h)$, where I is the current amplitude at +80 mV, I_{max} is the maximum current elicited by a saturating concentration of the ligand, [cNMP] is the ligand concentration, $K_{1/2}$ is the concentration of cNMP producing half-maximal current, and h is the Hill coefficient. For the L-cis-diltiazem (Sigma-Aldrich) experiments, 1 mM cGMP was used at +80 mV with or without 25 µM L-cis-diltiazem in the intracellular solution to confirm the formation of heteromeric CNG channels.

The Gibbs free energy, ΔG, of the overall reaction of CNG channel opening was calculated using the following equation, which assumed that the number of cGMP ligands contributing to the channel activation was designated by the Hill coefficient (Craven et al., 2008; Kusch et al., 2010), $\Delta G = -RT ln(1/K_{1/2}{}^h)$, where R is the gas constant, 1.987 $cal \cdot K^{-1} \cdot mol^{-1}$, and T is the temperature (298 K). Based on that equation, we calculated the phosphoinositide-induced energy change for the channel opening reaction, ΔΔG, using $\Delta\Delta G = \Delta G_{PIPn} - \Delta G_{cont} = RT ln[(K_{1/2,PIPn}{}^{h(PIPn)})/(K_{1/2,cont}{}^{h(cont)})]$, where cont (control) and PIP_n indicate the values before and after phosphoinositide treatment. Data parameters were expressed as mean ± SEM of n experiments unless otherwise indicated. Statistical significance was determined by using Student's t test (or a Mann–Whitney U test). For comparing multiple groups of experiments, one-way analysis of variance followed by all pairwise multiple comparisons (Tukey's test for the multiple comparisons) was applied; a P-value of <0.05 was considered significant.

We used fluctuation analysis to estimate $P_{o\ max}$ at saturation concentrations of cyclic nucleotide. Mean isochrone variances (σ^2) from 4–8 sweeps at a low and saturating concentration of cyclic nucleotide were calculated, respectively (Alvarez et al., 2002). Currents were low-pass filtered at 2 kHz and digitized at 25 kHz. Assuming binomial distribution, $P_{o\ max}$ was calculated using the following equation (Goulding et al., 1994): $P_{o\ max} = 1 - (\sigma_{max}{}^2/I_{max})/(\sigma_{low}{}^2/I_{low})$, where $\sigma_{max}{}^2$ and $\sigma_{low}{}^2$ are mean isochrone variances at saturating and low concentrations of cyclic nucleotides, respectively; I_{max} and I_{low} are mean macroscopic currents at corresponding concentrations of cyclic nucleotides. The $P_{o\ max}$ for cAMP was calculated based on $P_{o\ max}$ for cGMP multiplied by I_{max} cAMP/cGMP.

In addition, we used tetracaine, a known state-dependent blocker of CNG channels, to estimate the $P_{o\ max}$. Tetracaine binds to closed channels with nearly 1,000-fold greater affinity compared with open channels; thus, channels that spend more time in the open state are less sensitive to tetracaine block (Fodor et al., 1997). As described previously (Fodor et al., 1997; Liu and Varnum, 2005), we calculated the equilibrium constant for the allosteric transition (L) for cGMP-bound channels using the apparent affinity for tetracaine ($K_{1/2,tetracaine}$) and the following equation: $L_{cG} = K_{do}(K_{1/2,tetracaine} - K_{dc})/K_{dc}(K_{do} - K_{1/2,tetracaine})$.

In this equation, K_{dc} (220 nM) and K_{do} (170 µM) are dissociation constants for tetracaine binding to closed or open channels, respectively. $P_{o\ max}$ was calculated as $P_{o\ max} = L/(1 + L)$. The $P_{o\ max}$ for cAMP was also calculated using $P_{o\ max}$ for cGMP and I_{max} cAMP/cGMP.

Online supplemental material

Fig. S1 shows the effects of PIP_n on apparent cGMP affinity of homomeric CNGA1, CNGA2, and CNGA3 channels. Fig. S2 shows that disruption of the cytoskeleton by cyto D does not prevent PIP_3 regulation of cAMP efficacy for homomeric CNGA3 channels. Fig. S3 shows several CNGB3 truncations and mutations that do not prevent PIP_n regulation of CNGA3+CNGB3 channels. Online supplemental material is available at http://www.jgp.org/cgi/content/full/jgp.201210944/DC1.

RESULTS

C-terminal component for regulation of CNGA3 channels by phosphoinositides

To investigate the mechanisms responsible for regulation of cone CNG channels by phosphoinositides, we expressed human CNGA3 subunits alone or with human CNGB3 subunits in *X. laevis* oocytes. For photoreceptor CNG channels, cGMP is nearly a full agonist, whereas cAMP is a partial agonist; this difference in efficacy for cAMP and cGMP depends on how well the bound ligands are able to promote the allosteric conformational change associated with channel opening (Goulding et al., 1994; Gordon and Zagotta, 1995; Varnum et al., 1995). We evaluated the relative efficacy of cAMP versus cGMP by measuring the current at +80 mV elicited by saturating concentrations of the respective ligands (10 mM for cAMP, 1 mM for cGMP). Although the apparent cGMP affinity of homomeric CNGA3 channels was not significantly altered by PIP_3 (Brady et al., 2006) or PIP_2 (Fig. S1), we surprisingly observed that application of phosphoinositide analogues to the cytoplasmic face of excised inside-out patches produced a large increase in the maximal cAMP current. We found that 1 µM diC8-PI (3, 4, 5) P_3 (PIP_3) or 10 µM diC8-PI (4, 5) P_2 (PIP_2) elicited a similar increase in relative cAMP efficacy (Fig. 1, A and B; for simplicity, in subsequent text and figures diC8-PI (3, 4, 5) P_3 and diC8-PI (4, 5) P_2 are referred to as PIP_3 and PIP_2, respectively). Reversal of this effect was facilitated by 25 µg/ml poly-lysine (Fig. 1, A and B), which screens the negative charges of the phosphoinositides. Similar results were observed with application of a 10-fold higher concentration of PIP_3 (10 µM; fold increase in I_{max} cAMP/cGMP was 2.63 ± 0.13, $n = 4$) or with application of 10 µM natural PIP_2 (fold increase in I_{max} cAMP/cGMP was 2.24 ± 0.26, $n = 4$). The maximal

cGMP current for homomeric CNGA3 channels was not significantly altered by PIP_3 or PIP_2 (P = 0.463 for PIP_3, P = 0.437 for PIP_2). In contrast, for CNGA1 homomeric channels, PIP_3 or PIP_2 decreased relative cAMP efficacy (Fig. 1 C), which is consistent with the general inhibitory effect of these phosphoinositides on CNGA1 channel gating (Fig. S1). In addition, neither PIP_3 nor PIP_2 significantly altered the apparent cAMP affinity of homomeric CNGA3 channels (P > 0.05); $K_{1/2}$ cAMP was found to be 1.13 ± 0.02 mM (n = 8) before PIP_n application, 1.16 ± 0.06 mM (n = 4) after PIP_3, and 1.13 ± 0.04 mM (n = 4) after PIP_2. Endogenous phosphoinositides also may tune cAMP efficacy of CNGA3 channels: application of poly-lysine to control patches produced a small but significant decrease in I_{max} cAMP/cGMP, from 0.18 ± 0.01 before to 0.10 ± 0.01 after poly-lysine (n = 4; P < 0.05). For heteromeric CNGA3+CNGB3 channels, no significant change in cAMP efficacy was observed with exposure of membrane patches to PIP_3 and PIP_2 (I_{max} cAMP/cGMP was 0.27 ± 0.01 [n = 11] before PIP_n application, 0.27 ± 0.02 [n = 6] after PIP_2, and 0.30 ± 0.03 [n = 5] after PIP_3). Together, these results show that CNGA3, in the absence of CNGB3 subunits, exhibits a PIP_n-induced increase in cAMP efficacy.

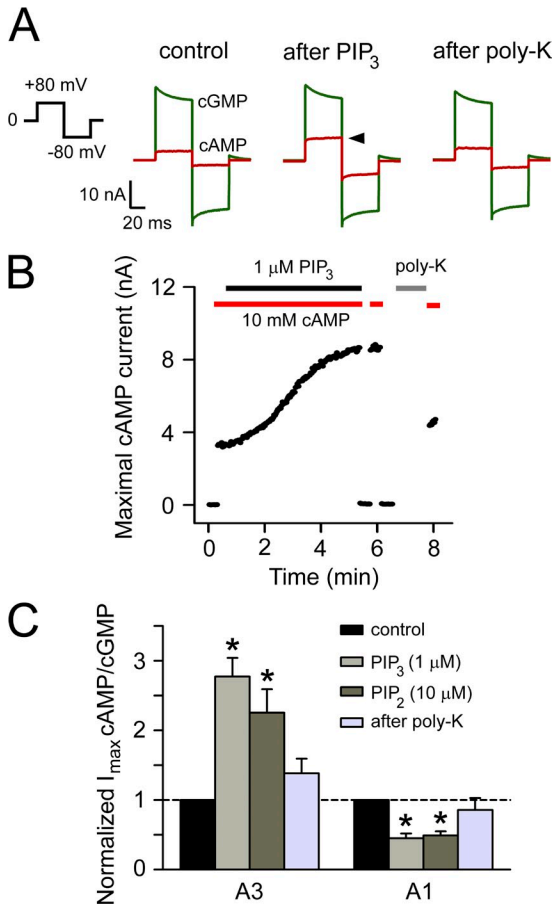

Figure 1. PIP_3 or PIP_2 potentiates relative cAMP efficacy for homomeric CNGA3 channels. (A) Representative current traces for homomeric CNGA3 channels, elicited by saturating concentrations of cGMP (1 mM, green) or cAMP (10 mM, red), before and after 1 μM PIP_3 (diC8-PIP_3) application, and after subsequent application of 25 μg/ml poly-lysine (poly-K). Currents were elicited by voltage steps from a holding potential of 0 mV to +80 mV, then to −80 mV and 0 mV (inset). Leak currents in the absence of cyclic nucleotide were subtracted. The arrowhead indicates I_{max} elicited by cAMP in the presence of PIP_3. (B) Time course for the change in maximal cAMP current (in 10 mM cAMP) induced by 1 μM PIP_3; also shown is reversal by 25 μg/ml poly-K. Horizontal bars indicate application of respective agents; currents were not recorded during poly-K application. (C) Summary illustrating PIP_3 (diC8-PIP_3)- or PIP_2 (diC8-PIP_2)-dependent changes in I_{max} cAMP/cGMP for CNGA3 and CNGA1 homomeric channels (normalized to control values before treatment). Data are from 10–12 (for PIP_3) or 3–4 (for PIP_2) independent experiments; *, P < 0.05 relative to before PIP_n application (control). The broken horizontal line refers to normalization to the value for I_{max} cAMP/cGMP of control patches. Error bars indicate mean ± SEM.

For CNG channels and hyperpolarization-activated CNG (HCN) channels, one key structural feature that contributes to cyclic-nucleotide selectivity and efficacy is a critical residue (D604 in CNGA1, D609 in CNGA3, and I636 in HCN2) within the Cα helix of the CNBD (Fig. 2 A; Varnum et al., 1995; Peng et al., 2004; Flynn et al., 2007; Zhou and Siegelbaum, 2007). Although other structural features in CNG channels can impart ligand-specific effects on gating (Young and Krougliak, 2004), this aspartic acid residue in CNGA1 is thought to interact more favorably with cGMP, while presenting a repulsive electrostatic interaction with cAMP, during the opening allosteric transition (Varnum et al., 1995; Sunderman and Zagotta, 1999). Using fluctuation analysis, we estimated the absolute $P_{o\ max}$ for wild-type CNGA3 channels in saturating concentrations of cGMP and cAMP to be 0.97 ± 0.01 (n = 10) and 0.13 ± 0.01 (n = 10), respectively. These $P_{o\ max}$ values for CNGA3 were similar to those obtained using a state-dependent block by tetracaine (Fodor et al., 1997; Liu and Varnum, 2005): ∼0.99 and ∼0.12, respectively. Fluctuation analysis confirmed that PIP_3 increased the absolute $P_{o\ max}$ cAMP to 0.37 ± 0.07 (n = 4), without significantly altering $P_{o\ max}$ cGMP (0.93 ± 0.01; n = 4). To determine whether the PIP_n-induced change in cAMP efficacy may involve changes in the interaction between cAMP and D609 in CNGA3, we altered this side chain via site-directed mutagenesis. As previously demonstrated (Peng et al., 2004), the D609K mutation increased relative cAMP efficacy (I_{max} cAMP/cGMP for D609K: 0.31 ± 0.02, n = 13) compared with wild-type channels (I_{max} cAMP/cGMP for wild-type CNGA3: 0.15 ± 0.01, n = 20; P < 0.001). For D609K channels, absolute $P_{o\ max}$ was estimated (using tetracaine block) to be 0.78 ± 0.01 (n = 7) for cGMP and 0.27 ± 0.02 (n = 7) for cAMP. D609K eliminated the PIP_n-dependent increase in cAMP efficacy for homomeric CNGA3 channels (Fig. 2, B and C). Furthermore, mutation D609M in CNGA3, similar to the equivalent CNGA1 D604M (Varnum et al., 1995), reversed ligand selectivity for

homomeric CNGA3 channels, making cAMP a better agonist than cGMP (I_{max} cAMP/cGMP for D609M: 2.83 ± 0.16, $n = 4$). For D609M channels, absolute $P_{o\ max}$ was estimated (using tetracaine block) to be 0.81 ± 0.02 ($n = 9$) for cAMP and 0.30 ± 0.02 ($n = 9$) for cGMP. Interestingly, PIP_3 elevated relative cGMP efficacy for D609M channels (Fig. 2, B and C), the inverse of the increase in cAMP efficacy observed for wild-type CNGA3 (Fig. 1 A).

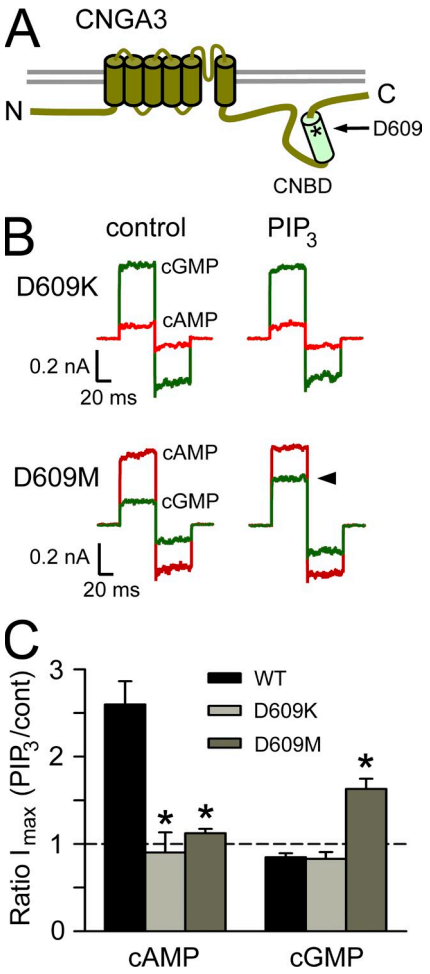

Figure 2. Mutation of critical ligand-discrimination residue (D609) within CNGA3 alters the PIP_3-induced increase in relative cAMP efficacy. (A) Diagram illustrating the basic topology of CNGA3 subunits (green), which are comprised of six transmembrane domains, with N- and C-terminal regions located on the intracellular side of the membrane. The light green cylinder represents the Cα helix of the CNBD. The asterisk indicates a critical ligand-discrimination residue, aspartic acid at position 609 (D609) within the CNBD. (B) Representative current traces elicited by 1 mM cGMP (green) or 10 mM cAMP (red) before and after 1 μM PIP_3, for CNGA3 D609K and D609M channels. The arrowhead indicates I_{max} elicited by cGMP in the presence of PIP_3. (C) Summary of the effects of 1 μM PIP_3 on the current elicited by saturating cAMP or cGMP, for CNGA3 wild-type, D609K, or D609M channels; *, $P < 0.05$ compared with wild-type channels, $n = 4$–5. The broken horizontal line refers to a ratio of one, equivalent to no change in the parameter after PIP_n application. Error bars indicate mean ± SEM.

Together, these results show that PIP_n can produce ligand-specific effects on channel gating, potentiating the ability of partial agonists to promote channel opening. The results are consistent with the interpretation that PIP_n can alter interactions between the channel and cyclic nucleotides during the conformational changes associated with channel opening.

Another important aspect of CNG channel ligand selectivity and for coupling the conformational change in the CNBD to channel opening is reorientation of the Cα helix (Varnum et al., 1995; Matulef et al., 1999; Matulef and Zagotta, 2002; Flynn et al., 2007; Taraska et al., 2009). We reasoned that the C-terminal region of the channel immediately distal to the Cα helix might play a role in mediating the effect of phosphoinositides on cAMP efficacy by influencing this reorientation. To test this idea, we generated serial deletions of the C-terminal region of CNGA3 (Fig. 3 A). Truncation of CNGA3 after amino acid 674 (675X) preserved the PIP_3-induced change in cAMP efficacy (Fig. 3 B). However, A3-655X channels exhibited less sensitivity to PIP_3, and A3-635X and A3-613X channels failed to show a PIP_3-dependent increase in cAMP efficacy (Fig. 3 B). For A3-635X, even a 10-fold higher concentration of PIP_3 (10 μM) produced no significant increase in cAMP efficacy (fold change after PIP_3 was 1.06 ± 0.03, $n = 4$; $P = 0.799$ compared with before PIP_3). The truncations alone produced only minor effects on the basic gating properties of CNGA3 channels (Table 1), which cannot easily account for the loss of PIP_n sensitivity. These results show that the PIP_n-mediated change in relative cAMP efficacy requires the post-CNBD region of CNGA3, including residues located between 635 and 655.

Phosphoinositides may regulate CNGA3 agonist efficacy through several possible mechanisms. For some channels, channel-interacting proteins appear to confer sensitivity to PIP_n regulation via an indirect mechanism. For other channels, poly-basic motifs present in cytoplasmic regions have been shown to be necessary for PIP_n regulation of channel function, possibly because they form direct electrostatic interactions with phosphoinositides or because they indirectly help couple PIP_n binding to changes in channel gating (for reviews see Gamper and Shapiro, 2007; Rosenhouse-Dantsker and Logothetis, 2007; Suh and Hille, 2008). Given the precedent provided by other channels, we hypothesized that conserved positively charged residues located in the post-CNBD region of CNGA3 may play a role in PIP_n regulation of cAMP efficacy. To test this idea, we generated mutations of these residues and investigated the effect of the mutations on PIP_n sensitivity. Neutralization of seven conserved lysines or arginines (C7K/R-A: K624A, K629A, R643A, R646A, K657A, K659A, R661A) within the C-terminal region of CNGA3 attenuated the PIP_3-induced change in cAMP efficacy (Fig. 3 C); these charge neutralizations did not significantly alter basic channel

gating properties compared with wild-type CNGA3 (Table 1). Neutralization of the three positively charged residues located between 655 and 675 (C3K/R-A: K657A, K659A, R661A) had no significant effect on the change in cAMP efficacy with PIP_3. Furthermore, neutralization of the two arginines located between 635 and 655 (RR-QQ: R643Q and R646Q) eliminated the PIP_3-induced increase in cAMP efficacy (Fig. 3 C). Somewhat paradoxically, charge reversal at these positions (RR-EE: R643E and R646E) reduced but did not eliminate the PIP_3-induced increase in cAMP efficacy, possibly because of more global changes in the structure of this region

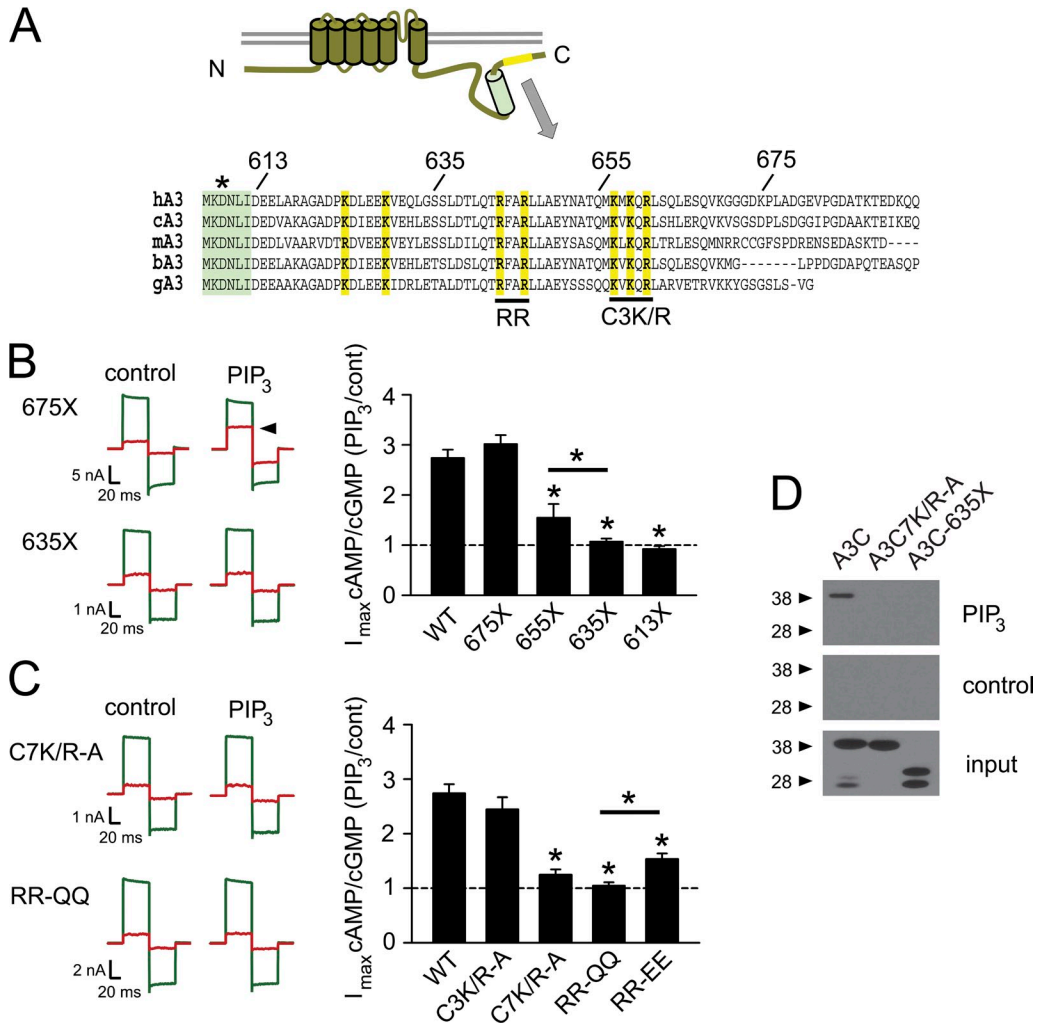

Figure 3. Change in relative cAMP efficacy after PIP_3 is dependent on the C-terminal region of CNGA3. (A) Schematic diagram showing sites of truncations and charge neutralizations within the human CNGA3 C-terminal region, and a sequence alignment of this region with orthologous CNGA3 proteins (canine, mouse, bovine, and gallus). Seven conserved lysines and arginines are highlighted in yellow. Bold nucleotides indicate residues in human A3 that were mutated in our study as well as related residues in A3 orthologues. The numbers above the sequence alignment indicate sites for introduced channels. Green highlighting indicates the distal region of the Cα helix. The asterisk indicates D609, as described in Fig. 2. (B) Representative current traces (left), elicited by 1 mM cGMP (green) or 10 mM cAMP (red) before and after 1 μM PIP_3, for CNGA3 675X and 635X channels. The right panel summarizes the effects of CNGA3 C-terminal deletions on PIP_3-induced increases in cAMP efficacy; *, $P < 0.05$ compared with wild-type channels, $n = 4–9$. The arrowhead indicates I_{max} elicited by cAMP in the presence of PIP_3. (C) Representative current traces (left), elicited by 1 mM cGMP (green) or 10 mM cAMP (red) before and after 1 μM PIP_3, for A3 C7K/R-A (K624A, K629A, R643A, R646A, K657A, K659A, R661A) and RR-QQ (R643Q, R646Q) channels. The right panel summarizes effects of mutations within the A3 C-terminal region on PIP_3-induced increases in cAMP efficacy; *, $P < 0.05$ compared with wild-type channels, $n = 4–6$. The broken horizontal lines refer to a ratio of one, equivalent to no change in the parameter after PIP_n application. (D) In vitro pull-down assay using PIP_3-bound or control agarose beads combined with GST fusion proteins representing the C-terminal region of CNGA3. Input proteins (bottom) and bound proteins (top) were identified by immunoblotting with anti-GST antibodies. A3C, C-terminal region of human CNGA3 from amino acids 612–694; A3C7K/R-A, C-terminal region with seven lysines and arginines neutralized to alanines, as highlighted in A; A3C-635X, C-terminal region of CNGA3 truncated at amino acid 635. Molecular weight markers (in kilodaltons) are shown on the left. Data are representative of four independent experiments. Error bars indicate mean ± SEM.

(see Hernandez et al., 2008). These results show that conserved residues R643 and R646 in CNGA3 play a role in mediating the PIP_n-dependent increase in cAMP efficacy. It is also likely that other structural features in the C-terminal region are necessary for PIP_n sensitivity.

One possible mechanism for the PIP_n-induced increase in cAMP efficacy is direct binding to the C-terminal region of the channel. To test for a potential direct channel–PIP_n interaction, we used a pull-down assay with PIP_3-linked agarose beads in combination with recombinant channel fragments expressed in *Escherichia coli* and subsequently purified using GST tags. This approach is not quantitative, and is not expected to accurately reflect conditions present at the plasma membrane with intact channels. In vitro PIP_3 binding was observed for the C-terminal channel fragment (A3C) containing amino acids 612–694 (Fig. 3 D). In addition, no binding was observed for control beads under these conditions. Charge neutralization of the conserved lysines and arginines in this region (A3C7K/R-A) or the 635X truncation (A3C-635X) both attenuated binding to PIP_3 beads. Collectively, these data imply that structural elements within the C-terminal region of CNGA3 are necessary for a component of PIP_n regulation. Also, the C-terminal region appears to be capable of supporting PIP_3 binding, at least in vitro. However, some caution is required for the interpretation of in vitro PIP_n-binding studies; other indirect mechanisms remain possible explanations for the C-terminal component of PIP_n action on the channel.

A plausible indirect mechanism for the link between phosphoinositides and the C-terminal region of CNGA3 is the cytoskeleton (Di Paolo and De Camilli, 2006; also see, for example, Otsuguro et al., 2008). We found that application of 10 µM cyto D, an agent that disrupts the actin-based cytoskeleton, to inside-out patches produced a decrease in cAMP efficacy for homomeric CNGA3 channels (Fig. S2, A and B). Truncation of the C-terminal region of CNGA3 (613X) mimicked and prevented further gating changes by cyto D (Fig. S2, A and B). This difference between wild-type and 613X channels suggests that deletion of the C-terminal region of CNGA3 uncouples the channel from the cytoskeleton. However, when we examined the effect of cyto D on the PIP_3 sensitivity of wild-type CNGA3, prior application of cyto D did not significantly alter the PIP_3-induced increase in relative cAMP efficacy (fold increase I_{max} cAMP/cGMP was 2.54 ± 0.27, n = 10; P = 0.307 compared with no cyto D; Fig. S2 C). Therefore, despite the convergent requirement for an intact C-terminal region for both the PIP_n- and cyto D–mediated changes in cAMP efficacy, the C-terminal component of PIP_n regulation is not prevented by disruption of the actin cytoskeleton, which suggests that a connection with the cytoskeleton is not required.

The cytoplasmic N-terminal region of CNGA3 supports PIP_n-dependent change in apparent cGMP affinity when unmasked by C-terminal truncation

How is the PIP_n-dependent change in apparent cGMP affinity for heteromeric CNGA3+CNGB3 channels mediated? Helping to address this question, we found that C-terminal truncation of CNGA3 after the CNBD (A3-613X) produced homomeric channels that exhibited a large increase in $K_{1/2}$ cGMP after PIP_3 application (Fig. 4, B and C). Enhanced PIP_n sensitivity was not observed after a less extensive C-terminal truncation (A3-635X). For A3-613X channels, the change in apparent cGMP affinity with phosphoinositides was analogous to,

TABLE 1

Gating parameters for CNGA3 mutations

CNGA3	$K_{1/2}$ cGMP (µM)	Hill coefficient	$P_{o\ max}$ cGMP	I_{max} cAMP/I_{max} cGMP
Wild type	9.29 ± 0.43 (18)	1.91 ± 0.04 (18)	0.97 ± 0.01 (10)	0.14 ± 0.01 (20)
613X	12.68 ± 0.99 (11)[a]	1.55 ± 0.09 (11)	0.93 ± 0.01 (4)	0.12 ± 0.01 (16)
635X	8.20 ± 0.57 (5)	2.00 ± 0.00 (5)	0.92 ± 0.01 (4)	0.18 ± 0.02 (5)
655X	8.83 ± 0.26 (3)	1.73 ± 0.10 (3)	0.94 ± 0.01 (4)	0.15 ± 0.02 (4)
675X	9.22 ± 0.55 (4)	1.88 ± 0.05 (4)	ND	0.15 ± 0.02 (6)
C7K/R-A	9.37 ± 0.29 (6)	2.00 ± 0.00 (6)	0.92 ± 0.01 (4)	0.16 ± 0.01 (6)
RR-QQ	7.45 ± 0.63 (3)	2.00 ± 0.00 (3)	0.94 ± 0.01 (3)	0.15 ± 0.01 (13)
RR-EE	8.29 ± 0.47 (4)	1.95 ± 0.05 (4)	0.93 ± 0.03 (4)	0.17 ± 0.01 (10)
P99L, A105P	5.30 ± 0.18 (7)[a]	2.00 ± 0.00 (7)	0.95 ± 0.01 (4)	0.21 ± 0.01 (7)[a]
ΔN (2-156)	9.16 ± 0.65 (9)	1.77 ± 0.07 (9)	ND	0.18 ± 0.01 (13)[a]
ΔN (2-156), 613X	15.75 ± 2.80 (6)[a]	1.66 ± 0.10 (6)	ND	0.10 ± 0.02 (6)
ΔN (51-107), 613X	11.14 ± 2.28 (4)	1.90 ± 0.06 (4)	ND	0.10 ± 0.01 (4)
N7R-A	8.89 ± 1.15 (4)	1.59 ± 0.18 (4)	ND	0.11 ± 0.01 (4)
N7R-A, 613X	16.36 ± 1.65 (6)[a]	1.82 ± 0.04 (6)	ND	0.10 ± 0.04 (4)
N5R-A, 613X	16.74 ± 0.98 (8)[a]	1.71 ± 0.05 (8)	ND	0.10 ± 0.01 (8)
N2R-A, 613X	16.10 ± 0.59 (4)[a]	1.68 ± 0.03 (4)	ND	0.11 ± 0.01 (4)

The numbers in parentheses after the gating parameters indicate the number of patches (n).
[a]Significant difference compared to wild-type CNGA3 channels (P < 0.05).

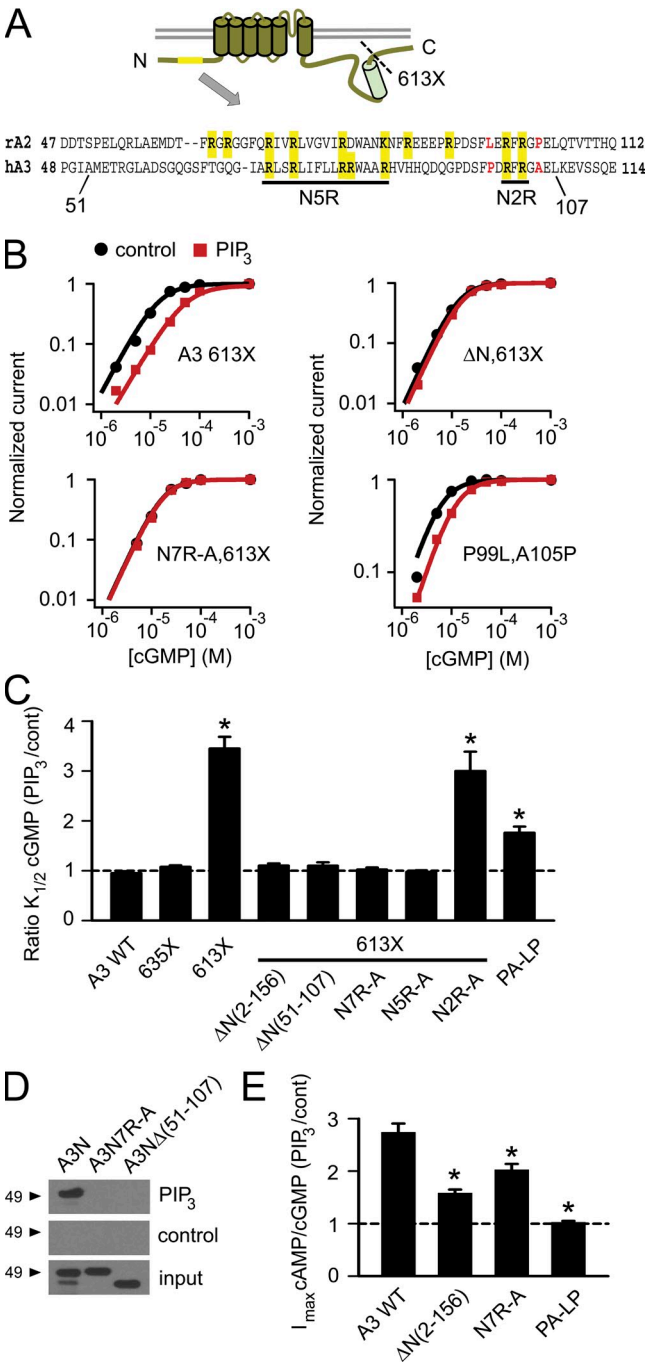

Figure 4. N-terminal region of CNGA3 can confer a PIP_n-dependent change in apparent cGMP affinity after C-terminal truncation. (A) Subunit diagram and sequence alignment of the N-terminal region of human CNGA3 and rat CNGA2 subunits. The residues highlighted in yellow are conserved arginines in this region of the channel. P99 and A105 of CNGA3, and the corresponding L97 and P103 of CNGA2, are in red. Bold nucleotides indicate residues in human A3 that were mutated in our study as well as related residues in the paralogous rat A2. (B) Representative cGMP concentration–response plots for activation of four different homomeric CNGA3 channels before and after 1 μM PIP_3: C-terminal deleted (A3-613X), combined N and C deletions (A3ΔN (51–107), 613X), N-terminal charge neutralizations (R72A, R75A, R81A, R82A, R86A, R101A, R103A) combined with C-terminal truncation (A3-N7R-A, 613X), or P99L, A105P (PA-LP) mutations. Currents were measured at +80 mV and were normalized to the maximum current elicited by a saturating concentration of cGMP. Continuous curves represent fits of the cGMP concentration–response relationship with the Hill equation. Hill parameters of the representative patches were as follows. For A3-613X, $K_{1/2}$ = 14.7 μM, h = 1.55 before PIP_3; $K_{1/2}$ = 50.9 μM, h = 1.4 after PIP_3. For A3 PA-LP, $K_{1/2}$ = 5.7 μM, h = 1.7 before PIP_3; $K_{1/2}$ = 11.4 μM, h = 1.7 after PIP_3. (C) Summary of PIP_3-dependent changes in $K_{1/2}$ cGMP for CNGA3 channels having the specific deletions and/or mutations shown; *, $P < 0.05$ compared with wild-type A3. (D) N-terminal domain of CNGA3 was expressed as a GST fusion protein and tested for PIP_3 binding in vitro by using PIP_3-agarose beads. A3N, N-terminal region (amino acids 1–164) of human CNGA3; A3N7R-A, seven arginines were neutralized to alanines within the N-terminal region; A3NΔ51-107, N-terminal region with amino acids 51–107 deleted. Molecular weight markers (in kilodaltons) are shown on the left. Data are representative of four independent experiments. (E) Deletions or charge neutralizations within the N-terminal region of CNGA3, A3 ΔN(2–156) or A3 N7R-A attenuated but did not eliminate the PIP_3-induced increase in relative cAMP efficacy (I_{max} cAMP/cGMP), whereas P99L, L105P (PA-LA) mutations in the N-terminal region eliminated this increase; *, $P < 0.05$ compared with wild-type A3. The broken horizontal lines refer to a ratio of one, equivalent to no change in the parameter after PIP_n application. Error bars indicate mean ± SEM.

but more pronounced than, that observed with A3+B3 channels (compare Figs. 4 and 5): $K_{1/2}$ cGMP for activation of A3-613X channels increased from 12.9 ± 3.3 μM (n = 11) to 47.4 ± 7.2 μM after PIP_3 (n = 7) and to 46.9 ± 10.2 μM after PIP_2 (n = 4). Because the N-terminal domain of CNG channels is considered one of the critical regions tuning channel sensitivity to cyclic nucleotides (Goulding et al., 1994; Gordon and Zagotta, 1995; Möttig et al., 2001) and has been shown previously (for CNGA2 and CNGA3) to bind PIP_3 in vitro (Brady et al., 2006), we engineered homomeric CNGA3 channels with both N- and C-terminal deletions. We found that the PIP_3-dependent change in $K_{1/2}$ observed with A3-613X channels was eliminated by complete N-terminal deletion (A3 ΔN [2–156], 613X). Moreover, a smaller deletion within the N-terminal region (A3 ΔN [51–107], 613X), which prevented PIP_3 binding in vitro (Brady et al., 2006), similarly eliminated the change of $K_{1/2}$ cGMP after PIP_3 application to the channels (Fig. 4, B and C).

We next asked whether conserved, positively-charged residues contribute to the N-terminal component for regulation of CNGA3 by phosphoinositides. When clusters of arginines in this region were neutralized (N7R-A: R72A, R75A, R81A, R82A, R86A, R101A, R103A), the PIP_3-induced decrease in apparent cGMP affinity observed for A3-613X channels was abolished (Fig. 4, B and C). For A3 N7R-A 613X, even application of a 10-fold higher concentration of PIP_3 (10 μM) produced no significant increase in $K_{1/2}$ cGMP (fold change after PIP_3 was 1.02 ± 0.05, n = 4; P = 0.887 compared with before PIP_3). Neutralization of the arginine cluster more distal to the transmembrane region (N5R-A) was

sufficient to eliminate the decrease in apparent cGMP affinity after PIP_3, but neutralizing the more proximal two arginines (N2R-A) produced channels that were not significantly different from A3-613X channels. Consistent with our previous work (Brady et al., 2006), an in vitro PIP_3 binding assay demonstrated that the N-terminal fragment of CNGA3 (A3N) was able to directly bind PIP_3; charge neutralizations in this region (A3N7R-A) attenuated binding to PIP_3 beads (Fig. 4 D), in parallel with their effects on PIP_3 regulation of channel cGMP sensitivity (Fig. 4, B and C). Together, these experiments suggest that in intact CNGA3 homomeric channels, a phosphoinositide-regulation module within the N-terminal cytoplasmic region is silent. However, when the distal C terminus of CNGA3 is deleted, this regulation module becomes functionally active, triggering a large decrease in apparent cGMP affinity for homomeric CNGA3 channels once PIP_3 or PIP_2 is bound.

The N-terminal region of human CNGA3 subunits previously has been shown to have a CaM binding site that is functionally silent (Grunwald et al., 1999; Peng et al., 2003a); this CaM-binding site overlaps with the region containing the putative N-terminal PIP_3-binding site (N5R) described here (Fig. 4 A). Grunwald et al. (1999) have shown previously that changing specific residues within the N-terminal domain of CNGA3, outside of the CaM-binding site, to those present in CNGA2 can unmask Ca^{2+}-CaM regulation of homomeric CNGA3 channels. Two key changes, P99L and A105P (Grunwald et al., 1999), are also present in CaM-sensitive chicken CNGA3 subunits (Bönigk et al., 1996), but not in CaM-insensitive CNGA3 subunits from other species. Consequently, we tested the idea that P99L and A105P mutations (PA-LP) might also unmask the phosphoinositide sensitivity of CNGA3 homomeric channels. As expected, the basal apparent cGMP affinity was increased for PA-LP channels compared with wild-type CNGA3 (Table 1). Similar to A3-613X, A3 PA-LP channels demonstrated a significant increase in $K_{1/2}$ cGMP after PIP_3 or PIP_2 application (see Fig. 7, B and C). Hill parameters for PIP_n modulation of CNGA3 PA-LP channels were as follows: $K_{1/2}$ = 5.3 ± 0.2 µM, h = 2 before PIP_n; $K_{1/2}$ = 9.4 ± 0.9 µM, h = 1.8 after PIP_3 (n = 7); and $K_{1/2}$ = 8.7 ± 0.4 µM, h = 1.7 after PIP_2 (n = 4). Likewise, A3-613X channels exhibited enhanced sensitivity to regulation by Ca^{2+}-CaM, demonstrating an approximately twofold increase (1.98 ± 0.20, n = 7) in $K_{1/2}$ cGMP after application of Ca^{2+}-CaM ($P < 0.01$, compared with wild-type CNGA3). Together, these results raise the possibility that interdomain coupling between N- and C-terminal regions may control the regulatory competency of the N-terminal domain of CNGA3, which can mediate the effects of CaM or phosphoinositides on channel activity.

Next we investigated whether the N-terminal domain of CNGA3 might influence the increase in cAMP efficacy with PIP_n that depends on structural features within the C-terminal region (the C-terminal regulatory module). CNGA3 N-terminal deletion (Δ2-156), or charge neutralizations within the critical N-terminal region (N7R-A) significantly reduced but did not eliminate the increase in cAMP efficacy with PIP_3 (Fig. 4 E). This indicates that the C-terminal component of PIP_n sensitivity does not require an intact N-terminal regulatory module. However, P99L and A105P mutations (PA-LP) within the N-terminal region of CNGA3 eliminated the effect of PIP_3 on cAMP efficacy (Fig. 4 E). Collectively, the results show that CNGA3 subunits present separable N and C regulatory modules supporting different types of sensitivity to PIP_n: a decrease in apparent cGMP affinity (the N component) or an increase in partial agonist efficacy (the C component). Each independent regulatory module can function in the absence of structural features necessary for action of the other module. Conversely, changes in the N or C domains (e.g., PA-LP or 613X, respectively) can dramatically tune the reciprocal regulatory component.

Both N- and C-terminal cytoplasmic regions of CNGA3 contribute to PIP_n regulation of heteromeric CNGA3+CNGB3 channels

The apparent cGMP affinity of heteromeric CNGA3+CNGB3 channels is sensitive to regulation by PIP_n (Bright et al., 2007). We found that 1 µM PIP_3 or 10 µM PIP_2 attenuated the currents elicited by application of 5 µM cGMP (Fig. 5 A), a subsaturating concentration of cGMP that approximates the dark steady-state level in vertebrate photoreceptors (Pugh et al., 1999; Fain et al., 2001). As previously described, cGMP dose–response relationships for activation of the heteromeric channels show that application of 1 µM PIP_3 shifted the $K_{1/2}$ cGMP ~1.5-fold to a higher concentration of ligand (Fig. 5 B, left; Bright et al., 2007). We found that higher concentrations of PIP_2 (10 µM) were able to produce a similar shift in the apparent affinity for cGMP (Fig. 5 B, right). The mean Hill parameters for PIP_n modulation of A3+B3 channels were as follows: $K_{1/2}$ = 13.5 ± 0.6 µM, h = 1.9 before PIP_n (n = 18); $K_{1/2}$ = 20.8 ± 1.4 µM, h = 1.6 after PIP_3 (n = 9); or $K_{1/2}$ = 23.4 ± 1.8 µM, h = 1.6 after PIP_2 (n = 9). At these concentrations of PIP_3 or PIP_2, we observed only a small decrease in the current at a saturating concentration of cGMP: I_{max} cGMP was 95.4 ± 2.8% (n = 9) after 1 µM PIP_3 and 85.3 ± 3.7% (n = 6) after 10 µM PIP_2 compared with initial values. Fig. 5 C shows the concentration–response relationship for the percent increase in $K_{1/2}$ cGMP produced by various concentrations of PIP_3, PIP_2, or natural PIP_2 applied to patches expressing heteromeric CNGA3+CNGB3 channels. These results indicate that A3+B3 channels may exhibit somewhat greater sensitivity to regulation by PIP_3 compared with PIP_2.

To determine whether the structural features necessary for regulation of homomeric CNGA3 channels by

phosphoinositides are also important for regulation of heteromeric CNG channels, we tested the effects of CNGA3 mutations and/or deletions on the PIP_3 and PIP_2 sensitivity of A3+B3 channels. For all subunit combinations, the formation of functional heteromeric channels at the plasma membrane were confirmed by sensitivity to block by L-cis-diltiazem, which serves as a reporter for incorporation of CNGB3 subunits into functional CNG channels (Gerstner et al., 2000; Peng et al., 2003b). Charge neutralizations within the critical N-terminal region of CNGA3 (N7R-A) significantly reduced but did not eliminate the reduction in apparent cGMP affinity by PIP_3 or PIP_2 for heteromeric CNGA3+CNGB3 channels (Fig. 6 B). Similarly, charge neutralizations in the C-terminal region of CNGA3 (RR-QQ) significantly reduced but did not eliminate the reduction in apparent cGMP affinity with PIP_3 or PIP_2 for heteromeric channels (Fig. 6 B). However, combining mutations in the N-terminal region (N7R-A) with mutations in the C-terminal region of CNGA3 (RR-QQ), each of which eliminated the respective N- and C-terminal components of PIP_n regulation for homomeric CNGA3 channels, gave rise to heteromeric channels that were insensitive to regulation by 10 µM PIP_2 or 1 µM PIP_3 (Fig. 6, A and B; *t* test for the effects of PIP_n on A3-N7R-A,RR-QQ+B3 channels; P = 0.618 for PIP_2 and P = 0.896 for PIP_3). For A3-N7R-A,RR-QQ+B3 channels, a 10-fold higher concentration of PIP_3 (10 µM) still produced no significant increase in $K_{1/2}$ cGMP (the percent change caused by PIP_3 was 2 ± 8%, n = 5; P = 0.930 compared with before PIP_3). These results indicate that both N- and C-terminal regions of CNGA3 contribute to PIP_n regulation of heteromeric CNGA3+CNGB3 channels.

A corollary to the results shown in Fig. 6 (A and B) is the implication that CNGB3 subunits cannot support PIP_n sensitivity in the absence of functional PIP_n-regulation modules in CNGA3. To further investigate this implication, we coexpressed CNGB3 subunits with CNGA1 or CNGA2 subunits. CNGA2-containing (olfactory) CNG channels previously have been shown to be sensitive to PIP_3 regulation (Spehr et al., 2002; Zhainazarov et al., 2004; Brady et al., 2006); deletion of amino acids 61–90 within the N-terminal region of CNGA2 generated homomeric A2 channels and heteromeric A2/B1b/A4 channels that were insensitive to PIP_3 (Brady et al., 2006). To isolate the possible influence of the CNGA3 subunit on PIP_n sensitivity of heteromeric channels, we used PIP_n-insensitive CNGA2 subunits with the 61–90 deletion (A2ΔN). We found that A2ΔN+B3 and A2ΔN+B1 channels were both insensitive to regulation by PIP_3. (Fig. 6, C and D). In contrast, coexpression of wild-type CNGA2 with CNGB3, CNGA1 with CNGB3, or CNGA3 with CNGB1 all formed PIP_3-sensitive channels (Fig. 6 D). Furthermore, CNGB3 subunits with extensive N- and C-terminal truncations (Δ2-205; Δ669-809), and/or charge-neutralizing mutations in other potential PIP_n-binding sites located in the S2-S3 loop, S4-S5 loop, or C-linker cytoplasmic regions of CNGB3, all preserved the PIP_n sensitivity of A3+B3 channels (Fig. S3). Overall, these results suggest that regulation of photoreceptor

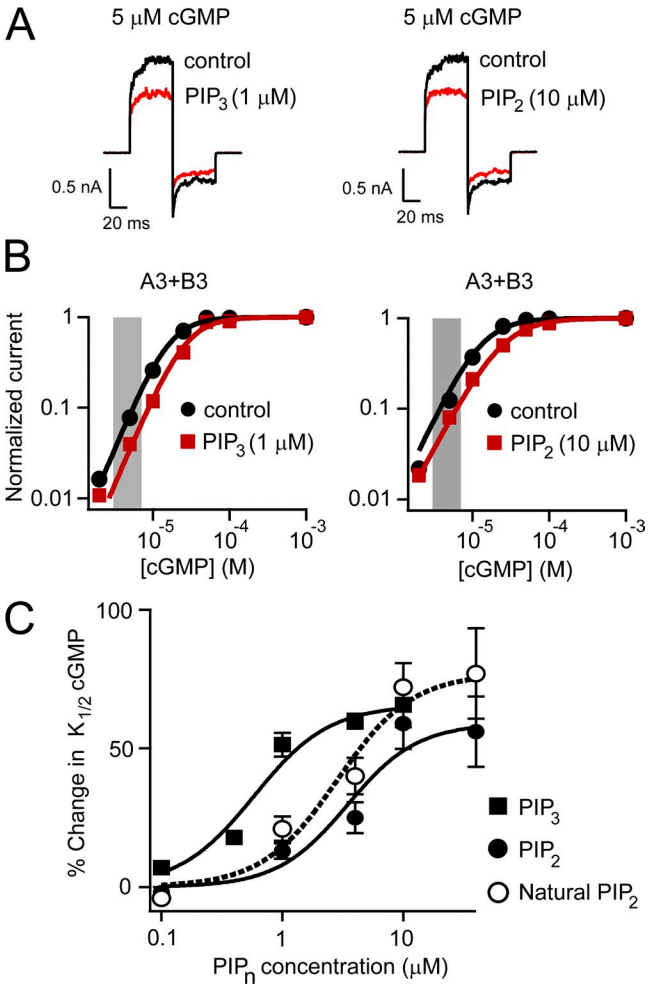

Figure 5. Heteromeric CNGA3+CNGB3 channels are inhibited by PIP_3 or PIP_2. (A) Representative current traces for heteromeric CNGA3+CNGB3 channels, elicited by subsaturating concentrations of cGMP (5 µM), before (black) and after (red) 1 µM PIP_3 or 10 µM PIP_2 application for ~5 min. (B) Representative dose–response relationships for the activation of heteromeric CNGA3+CNGB3 channels by cGMP before and after PIP_3 or PIP_2 application. The shadings indicate the approximate physiological range of intracellular cGMP levels within vertebrate photoreceptors in the dark. The Hill parameters for each representative patch were: $K_{1/2}$ cGMP = 16.1 µM, h = 2.05 before PIP_3; $K_{1/2}$ cGMP = 26.5 µM, h = 2.0 after PIP_3; $K_{1/2}$ cGMP = 12.8 µM, h = 1.8 before PIP_2; and $K_{1/2}$ cGMP = 24.5 µM, h = 1.6 after PIP_2. (C) Plot of percentage increase in $K_{1/2}$ cGMP for heteromeric A3+B3 channels at different concentrations of PIP_3 (closed squares), PIP_2 (closed circles), and natural PIP_2 (open circles; n = 4–5 for each PIP_n concentration). The PIP_n concentration–response relationships were fitted with the Hill equation, and the Hill parameters ($K_{1/2}$ and h) for each phosphoinositide species were as follows: 0.58 µM and 1.4 for PIP_3 (diC8-PIP_3), 3.44 µM and 1.5 for PIP_2 (diC8-PIP_2), and 2.84 µM and 1.4 for natural PIP_2. Error bars indicate mean ± SEM.

CNG channels by phosphoinositides is subunit specific: CNGA3 or CNGA1 subunits, but not CNGB3 or CNGB1 subunits, appear to confer PIP_n sensitivity upon heteromeric channels.

Intersubunit N–C interactions control regulation of cone CNGA3 channels by phosphoinositides

The results described here suggest that the C-terminal domain of CNGA3 can restrict an N-terminal component of PIP_n sensitivity; when the C-terminal domain was truncated (613X), then a robust change in $K_{1/2}$ cGMP after PIP_n application was revealed (Fig. 4, B and C). Similarly, mutations or deletions in the N-terminal domain of CNGA3 influenced the C-terminal component of PIP_n sensitivity (Fig. 4 E). Based on these observations, we hypothesized that interdomain N–C interactions involving CNGA3 subunits control the PIP_n sensitivity of cone CNG channels. Therefore, we sought to determine whether the coupling between N- and C-terminal regions that appears to regulate PIP_n sensitivity occurs only within the same subunit (intrasubunit) or between channel subunits (intersubunit). To address this question, we coexpressed CNGA3 subunits with distinct changes that each individually eliminated the increase in cAMP efficacy with PIP_n application (the C-terminal component of PIP_n sensitivity): one subunit with PA-LP mutations in the N-terminal region and one subunit with RR-QQ mutations in the C-terminal region. If the N-terminal PA-LP mutations silenced the C-terminal component of PIP_n sensitivity only within the same subunit (intrasubunit interaction), then the combination of these two insensitive subunits would produce a mixture of channels that remain insensitive to PIP_3. Conversely, if the N-terminal PA-LP mutations exerted an effect on the adjacent subunit (intersubunit interaction), then the mixture of channels formed by the combination of these subunits would produce some level of regulation of cAMP efficacy by PIP_3. In this scenario, regulation would be supported by complementary subunits via interaction of the normal N-terminal domain of RR-QQ subunits with the normal C-terminal domain of PA-LP subunits. For PA-LP+RR-QQ channels, we observed a small but significant increase in cAMP efficacy with PIP_3 compared with homomeric PA-LP and homomeric RR-QQ channels (Fig. 7 A). Assuming random subunit assembly and a binomial distribution of channel species, under these conditions the expected mean number of favorable intersubunit N–C interactions is only about one per channel (out of four possible). This outcome is consistent with an intersubunit N–C interaction for CNGA3 that regulates the C-terminal component of PIP_3 sensitivity.

We applied a similar approach to gain insight into how putative N–C coupling might control the N-terminal component of PIP_n sensitivity. As described in Fig. 4, the C-terminal truncation (613X) in CNGA3 unmasked the

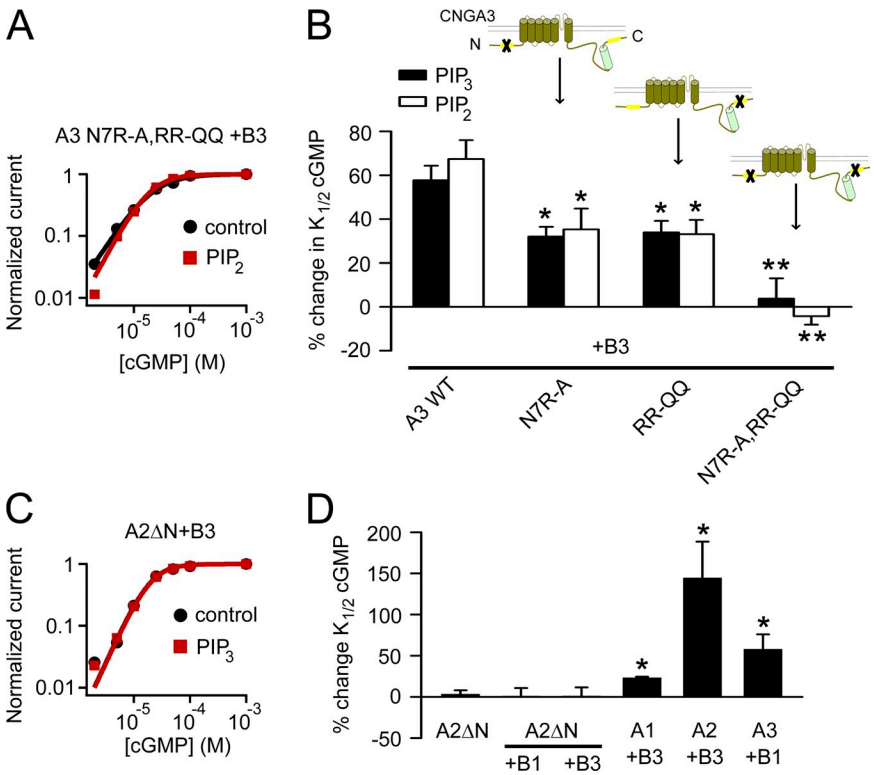

Figure 6. Both N- and C-terminal regions of CNGA3 subunits are important for modulation of heteromeric CNGA3+CNGB3 channels by PIP_3 or PIP_2. (A) Representative cGMP concentration–response plot showing the effect of 10 µM PIP_2 on A3+B3 heteromeric channels having N- (N7R-A) and C-terminal (RR-QQ) charge neutralizations within CNGA3. (B) Effects of PIP_3 (1 µM) and PIP_2 (10 µM) on heteromeric A3+B3 channels having specified mutations in A3 subunits. *, $P < 0.05$; **, $P < 0.001$ compared with wild-type A3+B3 for both PIP_3 and PIP_2. In the pairwise comparisons, statistically significant differences ($P < 0.05$) were also detected between A3N7R-A+B3 or A3 RR-QQ+B3 versus A3 N7R-A, RR-QQ+B3 channels. (C) Representative cGMP concentration–response relationship for activation of A2ΔN+B3 channels before (black) and after 1 µM PIP_3 (red). (D) Percentage change in $K_{1/2}$ cGMP after PIP_3 (1 µM) for various CNG channel subunit compositions. A2ΔN (Brady et al., 2006), A2ΔN+B1, A2ΔN+B3 channels showed no sensitivity to PIP_3, whereas PIP_3 produced a statistically significant increase in $K_{1/2}$ cGMP for A1+B3 ($n = 4$), A2+B3 ($n = 3$), and A3+B1 ($n = 4$) channels compared with A2ΔN+B3 or A2ΔN+B1 channels (*, $P < 0.05$). Error bars indicate mean ± SEM.

N-terminal component of PIP_n sensitivity, manifested as a large change in $K_{1/2}$ cGMP; charge neutralizations within the N-terminal region of CNGA3 (N7R-A) eliminated the PIP_n sensitivity of 613X channels. If the 613X truncation activates the N-terminal component of PIP_n sensitivity only within the same subunit (intrasubunit), then combining insensitive wild-type CNGA3 subunits with insensitive N7R-A,613X subunits would produce channels that remain insensitive to phosphoinositides. Conversely, if the 613X truncation activates the N-terminal regulatory component of an adjacent subunit (intersubunit), then the assembly of A3 wild-type subunits with N7R-A,613X subunits would be expected to produce some channels that exhibit a change in $K_{1/2}$ cGMP after PIP_3 application. Because the 613X truncation reduced channel expression levels and is expected to impair channel assembly (Zhong et al., 2002, 2003; Shuart et al., 2011), we injected a 5:1 ratio of N7R-A,613X to wild-type A3 cRNA into oocytes. Coexpression of N7R-A,613X with wild-type A3 produced channels exhibiting a small but significant increase in $K_{1/2}$ cGMP after PIP_3 (Fig. 7 B), which is consistent with an intersubunit interaction controlling the N-terminal component of PIP_n sensitivity.

To verify this finding, we more precisely controlled channel subunit arrangement by engineering concatenated cDNA constructs to produce tandem dimers of wild-type and N7R-A,613X subunits (Fig. 7 B). The tandem-dimer configuration of wild-type subunits (A3//A3) by itself did not enhance PIP_3 sensitivity. As expected, expression of tandem-dimer constructs encoding alternating head-to-tail assemblies of wild-type and N7R-A,613X subunits generated a more robust increase in $K_{1/2}$ cGMP after PIP_3 compared with random assembly of the respective subunits (Fig. 7 B). The fixed arrangement of subunits with tandem A3//N7R-A,613X heterodimer expression (Fig. 8, iv) is expected to produce two favorable intersubunit N–C interactions per channel (out of four possible), compared with a mean of about one favorable intersubunit N–C interaction per channel with random assembly of wild-type A3 and N7R-A,613X monomers. In agreement with the predicted stoichiometry of favorable N–C interactions for tandem A3//N7R-A,613X heterodimers, the magnitude of the change in the energetics of channel opening produced by PIP_3 ($\Delta\Delta G$) was 1.29 ± 0.08 kcal/mol, approximately half that of 613X homomeric channels (2.64 ± 0.26 kcal/mol). Overall, these results are consistent with the existence of intersubunit N–C interactions that control the two components of PIP_n sensitivity (N and C) in channels containing CNGA3 subunits (Fig. 8). Because assembly with CNGB3 subunits by necessity alters some of these N–C interactions via substitution (of B3 cytoplasmic domains for some A3 cytoplasmic domains), we propose a model where CNGB3 tunes the regulatory features of CNGA3 (Fig. 8, v), producing heteromeric channels that exhibit a change in $K_{1/2}$ cGMP with changes in PIP_3 or PIP_2 levels.

DISCUSSION

Phosphoinositides modulate the function of a wide range of different ion channels, but for many channel types little is known about the underlying molecular mechanisms. In the present study, we have identified features and mechanisms fundamental for phosphoinositide regulation of cone CNG channel ligand sensitivity. For both cone and rod CNG channels, our results show that the A subunits likely represent the principal subunits supporting PIP_n regulation, whereas the B subunits are not sufficient to confer regulation when combined with PIP_n-insensitive A subunits. This interpretation applies also to olfactory CNG channels, where the A2 subunits support PIP_n regulation, but A4 and B1b subunits do not (Brady et al., 2006). Channels formed by CNGA3 subunits exhibit two separable components for regulation of channel gating by PIP_2 or PIP_3, which is reminiscent of the dual effect of PIP_2 regulation of

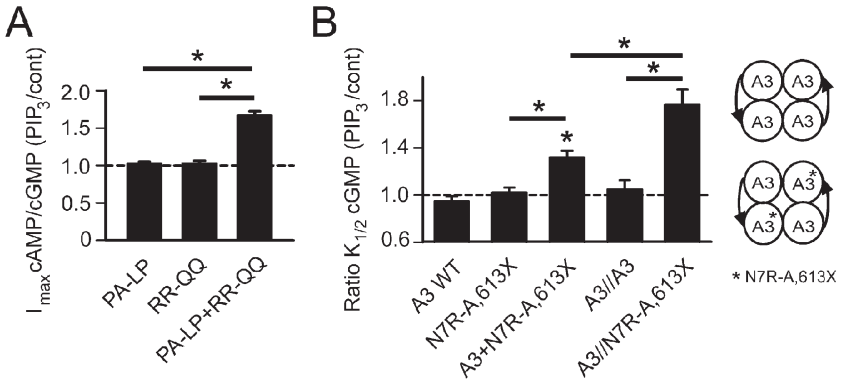

Figure 7. Intersubunit N–C coupling controls phosphoinositide sensitivity of CNGA3 channels. (A) Coexpression of PA-LA subunits with RR-QQ subunits, both of which individually form channels insensitive to 1 µM PIP_3 regarding cAMP efficacy, generated channels that were sensitive to PIP_3. The I_{max} cAMP/cGMP (PIP_3/control) for coexpression of A3 PA-LA with A3 RR-QQ was 1.67 ± 0.06 ($n = 6$, $P < 0.001$). (B) Coexpression of A3 wild type (WT) and A3 N7R-A,613X subunits generated channels that exhibited an increased $K_{1/2}$ cGMP after 1 µM PIP_3 application. Channels formed by A3 WT//A3 N7R-A,613X tandem dimers exhibited enhanced sensitivity to PIP_3-induced inhibition of apparent cGMP affinity. Ratio $K_{1/2}$ cGMP (PIP_3/control) was significantly greater for A3//A3 N7R-A,613X dimers ($n = 4$) compared with channels formed by coexpression of A3 with A3-N7R-A,613X ($n = 8$; $P < 0.05$). The broken horizontal lines refer to a ratio of one, equivalent to no change in the parameter after PIP_n application. Error bars indicate mean ± SEM.

several other related channels (Flynn and Zagotta, 2011; Rodriguez-Menchaca et al., 2012; Abderemane-Ali et al., 2012). First, cAMP efficacy for homomeric CNGA3 channels is enhanced by phosphoinositides and reduced by application of poly-lysine. This component depends on structural features located in the C-terminal region after the CNBD, and is influenced by a critical ligand discrimination residue in the CNBD. Binding of PIP_3 or PIP_2 to the channel, or to a channel-associated protein, may facilitate the ability of the CNBD to accommodate the partial agonist cAMP (or cGMP for D609M channels) during channel activation. A second component is mediated by the N-terminal region of CNGA3, which can confer a decrease in apparent cGMP affinity when combined with C-terminal truncation or assembly with CNGB3 subunits. Neutralization of conserved positively charged residues in each region eliminated each component of phosphoinositide sensitivity. Furthermore, both N- and C-terminal regions contribute to phosphoinositide regulation of heteromeric CNGA3+CNGB3 channels. However, in the context of heteromeric channels, the C-terminal component supports a change in $K_{1/2}$ cGMP rather than a change in cAMP efficacy. In addition, PIP_n effects on cone CNG channel gating were relatively stable, reversing slowly during washout, but reversal was accelerated by poly-lysine.

The two regions in CNGA3 shown here to be critical for PIP_n regulation may represent direct PIP_n binding sites, or, alternatively, be essential for communicating PIP_n binding elsewhere into changes in channel gating, thus stabilizing the closed state relative to the open state

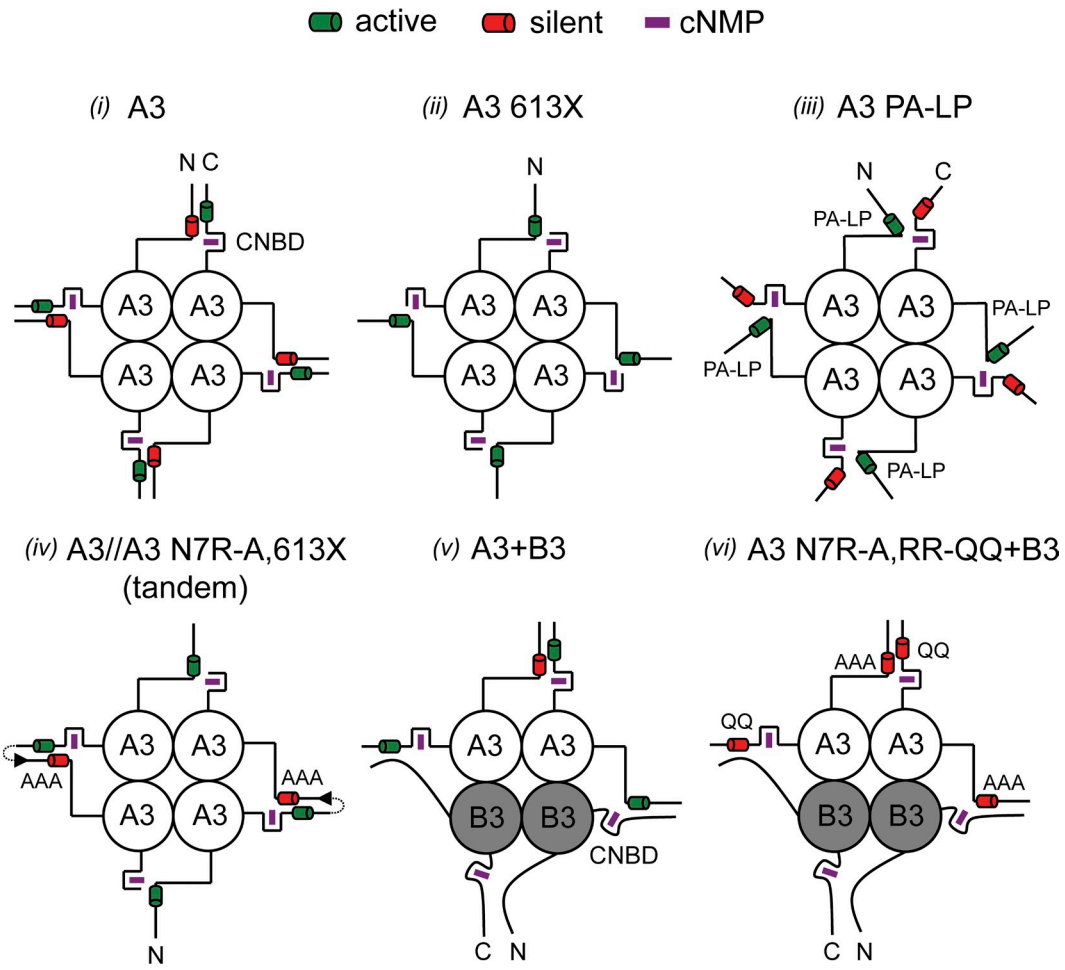

Figure 8. Model for tuning phosphoinositide sensitivity of cone CNG channels via intersubunit interactions. Six scenarios here illustrate how proposed N–C interactions between channel subunits may control PIP_n regulation. Two regulatory modules are located within the N- and C-terminal regions of CNGA3 subunits, respectively. These PIP_n-regulation modules can be silenced (red) or activated (green) due to changes in intersubunit interactions. (i) One component involves the C-terminal region of CNGA3, which is necessary for a PIP_n-dependent increase in cAMP efficacy. (ii and v) The other component, manifested as a decrease in apparent cGMP affinity, requires the N-terminal region of CNGA3 and is unmasked either by deletion of the C-terminal region (ii) or by assembly with CNGB3 subunits (v). (iii) PA-LP mutations in CNGA3 also alter N–C coupling, thereby activating the N module and silencing the C module. (iv) The PIP_n-regulation competency of channels formed by A3//A3 N7R-A,613X tandem dimers supports an intersubunit N–C interaction. (vi) In addition, PIP_n regulation of heteromeric CNGA3+CNGB3 channels depends on N and C regulatory modules in CNGA3.

of the channel. If one or both of these regions provide direct binding sites for phosphoinositides, the lack of pronounced PIP_n specificity and the loss of PIP_n sensitivity with CNGA3 positive-charge neutralizations are both consistent with electrostatic interactions between the channel and phosphoinositides. Mutations in CNGA3 that eliminated components of PIP_n regulation are unlikely to arise from a generalized allosteric destabilization of PIP_n binding, as none of the changes dramatically altered channel gating in the absence of phosphoinositides (Table 1). The lack of response to PIP_n for these mutations could arise from a change in PIP_n efficacy, a large decrease in sensitivity to PIP_n, or both. The CNGA3 N-terminal regulatory module is homologous to the overlapping CaM and putative PIP_3 binding site present in the N-terminal region of CNGA2 subunits (Grunwald et al., 1999; Brady et al., 2006). Consistent with previous studies showing that mutations outside the functionally silent, N-terminal CaM-binding site in CNGA3 can unmask CaM sensitivity (Grunwald et al., 1999), similar mutations (PA-LP) in CNGA3 also unmask PIP_n sensitivity. We propose that these mutations activate the N-terminal regulatory module of CNGA3 by altering coupling between N- and C-terminal domains of the channel.

The C-terminal component of PIP_n sensitivity appears to be unique to CNGA3 channels: it is not observed with either CNGA1 or CNGA2 homomeric channels, despite extensive sequence homology in the post-CNBD region. Our results are in several ways consistent with the simple scenario where the C-terminal region of CNGA3 provides a binding site for PIP_2 or PIP_3, as channel regulation and in vitro phosphoinositide binding are both disrupted by mutations of conserved positively charged residues. Conversely, likely structural constraints for the C-terminal domain make mechanisms that involve direct PIP_n binding seem less plausible for the C-terminal regulatory module compared with the N-terminal regulatory module. First, structures of related C-terminal fragments from HCN channels having homologous cyclic nucleotide-binding domains (Zagotta et al., 2003; Flynn et al., 2007) suggest that the post-CNBD region is distant from the plasma membrane, which seemingly precludes direct interactions with phosphoinositides. However, these structures present a static picture of the homologous C-terminal region that may not represent all possible configurations. For example, a putative PIP_2-binding site in the distal post-CNBD region of HERG channels has been identified (Bian and McDonald, 2007). Second, the post-CNBD region of CNGA3 is thought to form homotypic interactions via a C-terminal leucine zipper (CLZ; Zhong et al., 2002). These interactions are proposed to help control subunit assembly (Zhong et al., 2002, 2003; Shuart et al., 2011). It is not known if the CLZ coiled-coil bundle is a static or dynamic arrangement, but it could potentially restrict this region from direct interactions with phosphoinositides in the plasma membrane.

Instead, we favor an indirect mechanism for the C-terminal component of PIP_n sensitivity, where the region between amino acids 635 and 655 of CNGA3 is necessary to translate PIP_n binding—to a different site in CNGA3 or to a channel-associated protein—into a conformational change that modifies channel gating. It appears unlikely that the N-terminal regulatory module of CNGA3 represents that site, or that a combined "clamshell" phosphoinositide-binding site is formed by parts of the N- and C-terminal cytoplasmic domains of CNGA3. Note that CNGA3 N-terminal deletion, or N-terminal charge neutralizations, both leave intact the C-terminal component of PIP_n regulation. Also, CNGA3 635X lacks the C-terminal component, yet still masks the N-terminal component of PIP_n regulation in these channels. Instead, the results are consistent with the presence of two separable regulatory modules. Potential channel-interacting proteins that might indirectly mediate the C-terminal component of PIP_n regulation include Grb14, which has been shown recently to interact with the post-CNBD region of CNGA1 (Gupta et al., 2010). Grb14 processes a pleckstrin homology domain, and Grb14-PIP_3 complexes have been detected in retinal lysates after insulin stimulation (Rajala et al., 2005). Also, an unspecified tyrosine kinase is thought to directly associate with rod and cone photoreceptor CNG channels (Molokanova et al., 1999; Chae et al., 2007). In addition, localization of rod photoreceptor CNG channels has been shown to depend on interactions with elements of the cytoskeleton, including ankyrin G (Kizhatil et al., 2009). For NMDA receptors and TRPC4α channels, interaction with the actin cytoskeleton is necessary for PIP_2 regulation of channel function (Michailidis et al., 2007; Otsuguro et al., 2008). However, we found that actin cytoskeleton disruption did not prevent the PIP_n-dependent increase in cAMP efficacy for CNGA3 channels (Fig. S2). Another possible alternative PIP_n binding site not examined in the present study is the C-linker region of CNGA3. For related SpIH channels, one component of PIP_2 regulation depends on positively charged residues in the A′ helix of the C-linker region (Flynn and Zagotta, 2011). Related to this possibility, we have shown previously that in vitro CaM binding to the C-linker region of CNGA4 subunits is blocked by prior application of PIP_3 (Brady et al., 2006).

Our results suggest that intersubunit coupling involving N- and C-terminal cytoplasmic regions of CNGA3 helps control channel sensitivity to PIP_n regulation. Interdomain N–C interactions are characteristic of CNG channels and have been shown previously to be important for channel assembly, gating, and/or regulation (Gordon et al., 1997; Varnum and Zagotta, 1997; Rosenbaum and Gordon, 2002; Trudeau and Zagotta, 2002; Zheng et al., 2003; Michalakis et al., 2011). We propose a model where intersubunit interactions control the competency of the respective regulatory modules present in

the N- and C-terminal regions of CNGA3. Assembly of CNGB3 with CNGA3 subunits alters some of these interactions, thereby tuning the phosphoinositide sensitivity of the channels. Similarly, regulation of channel gating by N–C interactions has been described recently for related HERG channels, including a proposed interaction between the N-terminal domain and the homologous CNBD of HERG (Gustina and Trudeau, 2011; Muskett et al., 2011). In addition to CLZ interactions among C-terminal domains, CNG channels are thought to make intersubunit contacts between C-linker regions of adjacent subunits similar to those present in related HCN channels (Craven and Zagotta, 2004; Craven et al., 2008). For cone CNG channels, the precise intersubunit contacts and physical mechanisms responsible for N–C coupling related to PIP_n regulation remain to be determined.

The physiological impact of phosphoinositide regulation on photoreceptor CNG channel function is not well understood. For olfactory receptor neurons, PI3K activity has been shown to modulate odorant signaling, in part via PIP_3-dependent regulation of olfactory CNG channel ligand sensitivity (Spehr et al., 2002; Zhainazarov et al., 2004; Brady et al., 2006; Ukhanov et al., 2011). Some evidence indicates that photoreceptor phosphoinositide concentrations change under light, circadian, and paracrine control, and that these changes may influence photoreceptor function and health. Enzymes involved in PIP_n synthesis/metabolism are known to be located in the photoreceptor outer segment. For example, PI3K activity has recently been shown to contribute to rod photoreceptor function (Ivanovic et al., 2011a) and to be essential for cone photoreceptor viability (Ivanovic et al., 2011b). Light, insulin receptor activation, and tyrosine phosphorylation of outer segment proteins can regulate the plasma-membrane localization and activity of PIP_n kinases (Guo et al., 2000; Rajala and Anderson, 2001; Huang et al., 2011; Ivanovic et al., 2011a). A robust increase in outer segment PIP_3 levels after light exposure has been reported via GFP-tagged Akt1-PH domain localization in transgenic rod photoreceptors (Li et al., 2008). In addition to potential neuroprotective effects, local production or metabolism of phosphoinositides may contribute to modulation of phototransduction (Womack et al., 2000; He et al., 2004). Furthermore, PI3K activity has also been demonstrated to play a role in circadian outputs in photoreceptors (Ko et al., 2009). Changes in PIP_2 levels also may be critical for paracrine signaling pathways: somatostatin receptors in avian cone photoreceptors have been linked to a transient increase in CNG channel ligand sensitivity that depends on the phospholipase C activation (Chen et al., 2007). Finally, intracellular calcium concentration has been shown to be both an input and an output signal for changes in phosphoinositide levels (Gamper and Shapiro, 2007), including, for example, Ca^{2+}-dependent stimulation of PIP_2 synthesis via neuronal calcium sensor-1 (NCS-1; Zhao et al., 2001; Zheng et al., 2005; Winks et al., 2005). We speculate that PIP_n regulation may contribute to adjustments of CNG channel ligand sensitivity on a slow time scale (via paracrine or circadian inputs) and possibly on a faster time scale via light- and/or calcium-dependent changes in phosphoinositide metabolism.

This paper is dedicated to the memory of Dr. Louis Graham.

We thank Elizabeth Rich for excellent technical support; Dr. King-Wai Yau for sharing human CNGA3 cDNA; Dr. William Zagotta for sharing CNGA1, CNGA2, and CNGB1 cDNAs; Dr. Scott Bright for performing pilot experiments; and Drs. Pete Meighan, Starla Meighan, and Tshering Sherpa for constructive input.

Research described here was supported by a grant from the National Institutes of Health (EY12836).

Sharona E. Gordon served as editor.

Submitted: 4 December 2012
Accepted: 21 February 2013

REFERENCES

Abderemane-Ali, F., Z. Es-Salah-Lamoureux, L. Delemotte, M.A. Kasimova, A.J. Labro, D.J. Snyders, D. Fedida, M. Tarek, I. Baró, and G. Loussouarn. 2012. Dual effect of phosphatidyl (4,5)-bisphosphate PIP2 on Shaker K+ channels. *J. Biol. Chem.* 287:36158–36167. http://dx.doi.org/10.1074/jbc.M112.382085

Alvarez, O., C. Gonzalez, and R. Latorre. 2002. Counting channels: a tutorial guide on ion channel fluctuation analysis. *Adv. Physiol. Educ.* 26:327–341.

Bian, J.-S., and T.V. McDonald. 2007. Phosphatidylinositol 4,5-bisphosphate interactions with the HERG K(+) channel. *Pflugers Arch.* 455:105–113. http://dx.doi.org/10.1007/s00424-007-0292-5

Bönigk, W., F. Müller, R. Middendorff, I. Weyand, and U.B. Kaupp. 1996. Two alternatively spliced forms of the cGMP-gated channel alpha-subunit from cone photoreceptor are expressed in the chick pineal organ. *J. Neurosci.* 16:7458–7468.

Bradley, J., W. Bönigk, K.-W. Yau, and S. Frings. 2004. Calmodulin permanently associates with rat olfactory CNG channels under native conditions. *Nat. Neurosci.* 7:705–710. http://dx.doi.org/10.1038/nn1266

Brady, J.D., E.D. Rich, J.R. Martens, J.W. Karpen, M.D. Varnum, and R.L. Brown. 2006. Interplay between PIP3 and calmodulin regulation of olfactory cyclic nucleotide-gated channels. *Proc. Natl. Acad. Sci. USA.* 103:15635–15640. http://dx.doi.org/10.1073/pnas.0603344103

Bright, S.R., E.D. Rich, and M.D. Varnum. 2007. Regulation of human cone cyclic nucleotide-gated channels by endogenous phospholipids and exogenously applied phosphatidylinositol 3,4,5-trisphosphate. *Mol. Pharmacol.* 71:176–183. http://dx.doi.org/10.1124/mol.106.026401

Burns, M.E., and V.Y. Arshavsky. 2005. Beyond counting photons: trials and trends in vertebrate visual transduction. *Neuron.* 48:387–401. http://dx.doi.org/10.1016/j.neuron.2005.10.014

Chae, K.-S., G.Y.-P. Ko, and S.E. Dryer. 2007. Tyrosine phosphorylation of cGMP-gated ion channels is under circadian control in chick retina photoreceptors. *Invest. Ophthalmol. Vis. Sci.* 48:901–906. http://dx.doi.org/10.1167/iovs.06-0824

Chen, S.-K., G.Y.-P. Ko, and S.E. Dryer. 2007. Somatostatin peptides produce multiple effects on gating properties of native cone photoreceptor cGMP-gated channels that depend on circadian phase and previous illumination. *J. Neurosci.* 27:12168–12175. http://dx.doi.org/10.1523/JNEUROSCI.3541-07.2007

Crary, J.I., D.M. Dean, W. Nguitragool, P.T. Kurshan, and A.L. Zimmerman. 2000. Mechanism of inhibition of cyclic

nucleotide-gated ion channels by diacylglycerol. *J. Gen. Physiol.* 116:755–768. http://dx.doi.org/10.1085/jgp.116.6.755

Craven, K.B., and W.N. Zagotta. 2004. Salt bridges and gating in the COOH-terminal region of HCN2 and CNGA1 channels. *J. Gen. Physiol.* 124:663–677. http://dx.doi.org/10.1085/jgp.200409178

Craven, K.B., and W.N. Zagotta. 2006. CNG and HCN channels: two peas, one pod. *Annu. Rev. Physiol.* 68:375–401. http://dx.doi.org/10.1146/annurev.physiol.68.040104.134728

Craven, K.B., N.B. Olivier, and W.N. Zagotta. 2008. C-terminal movement during gating in cyclic nucleotide-modulated channels. *J. Biol. Chem.* 283:14728–14738. http://dx.doi.org/10.1074/jbc.M710463200

Di Paolo, G., and P. De Camilli. 2006. Phosphoinositides in cell regulation and membrane dynamics. *Nature.* 443:651–657. http://dx.doi.org/10.1038/nature05185

Ding, X.-Q., A. Matveev, A. Singh, N. Komori, and H. Matsumoto. 2012. Biochemical characterization of cone cyclic nucleotide-gated (CNG) channel using the infrared fluorescence detection system. *Adv. Exp. Med. Biol.* 723:769–775. http://dx.doi.org/10.1007/978-1-4614-0631-0_98

Fain, G.L., H.R. Matthews, M.C. Cornwall, and Y. Koutalos. 2001. Adaptation in vertebrate photoreceptors. *Physiol. Rev.* 81:117–151.

Flynn, G.E., and W.N. Zagotta. 2011. Molecular mechanism underlying phosphatidylinositol 4,5-bisphosphate-induced inhibition of SpIH channels. *J. Biol. Chem.* 286:15535–15542. http://dx.doi.org/10.1074/jbc.M110.214650

Flynn, G.E., K.D. Black, L.D. Islas, B. Sankaran, and W.N. Zagotta. 2007. Structure and rearrangements in the carboxy-terminal region of SpIH channels. *Structure.* 15:671–682. http://dx.doi.org/10.1016/j.str.2007.04.008

Fodor, A.A., S.E. Gordon, and W.N. Zagotta. 1997. Mechanism of tetracaine block of cyclic nucleotide-gated channels. *J. Gen. Physiol.* 109:3–14. http://dx.doi.org/10.1085/jgp.109.1.3

Gamper, N., and M.S. Shapiro. 2007. Regulation of ion transport proteins by membrane phosphoinositides. *Nat. Rev. Neurosci.* 8:921–934. http://dx.doi.org/10.1038/nrn2257

Gerstner, A., X. Zong, F. Hofmann, and M. Biel. 2000. Molecular cloning and functional characterization of a new modulatory cyclic nucleotide-gated channel subunit from mouse retina. *J. Neurosci.* 20:1324–1332.

Gordon, S.E., and W.N. Zagotta. 1995. Localization of regions affecting an allosteric transition in cyclic nucleotide-activated channels. *Neuron.* 14:857–864. http://dx.doi.org/10.1016/0896-6273(95)90229-5

Gordon, S.E., D.L. Brautigan, and A.L. Zimmerman. 1992. Protein phosphatases modulate the apparent agonist affinity of the light-regulated ion channel in retinal rods. *Neuron.* 9:739–748. http://dx.doi.org/10.1016/0896-6273(92)90036-D

Gordon, S.E., J. Downing-Park, B. Tam, and A.L. Zimmerman. 1995a. Diacylglycerol analogs inhibit the rod cGMP-gated channel by a phosphorylation-independent mechanism. *Biophys. J.* 69:409–417. http://dx.doi.org/10.1016/S0006-3495(95)79913-1

Gordon, S.E., J. Downing-Park, and A.L. Zimmerman. 1995b. Modulation of the cGMP-gated ion channel in frog rods by calmodulin and an endogenous inhibitory factor. *J. Physiol.* 486:533–546.

Gordon, S.E., M.D. Varnum, and W.N. Zagotta. 1997. Direct interaction between amino- and carboxyl-terminal domains of cyclic nucleotide-gated channels. *Neuron.* 19:431–441. http://dx.doi.org/10.1016/S0896-6273(00)80951-4

Goulding, E.H., G.R. Tibbs, and S.A. Siegelbaum. 1994. Molecular mechanism of cyclic-nucleotide-gated channel activation. *Nature.* 372:369–374. http://dx.doi.org/10.1038/372369a0

Grunwald, M.E., H. Zhong, J. Lai, and K.W. Yau. 1999. Molecular determinants of the modulation of cyclic nucleotide-activated channels by calmodulin. *Proc. Natl. Acad. Sci. USA.* 96:13444–13449. http://dx.doi.org/10.1073/pnas.96.23.13444

Guo, X.X., Z. Huang, M.W. Bell, H. Chen, and R.E. Anderson. 2000. Tyrosine phosphorylation is involved in phosphatidylinositol 3-kinase activation in bovine rod outer segments. *Mol. Vis.* 6:216–221.

Gupta, V.K., A. Rajala, R.J. Daly, and R.V.S. Rajala. 2010. Growth factor receptor-bound protein 14: a new modulator of photoreceptor-specific cyclic-nucleotide-gated channel. *EMBO Rep.* 11:861–867. http://dx.doi.org/10.1038/embor.2010.142

Gustina, A.S., and M.C. Trudeau. 2011. hERG potassium channel gating is mediated by N- and C-terminal region interactions. *J. Gen. Physiol.* 137:315–325. http://dx.doi.org/10.1085/jgp.201010582

He, F., M. Mao, and T.G. Wensel. 2004. Enhancement of phototransduction g protein-effector interactions by phosphoinositides. *J. Biol. Chem.* 279:8986–8990. http://dx.doi.org/10.1074/jbc.M311488200

Hernandez, C.C., O. Zaika, and M.S. Shapiro. 2008. A carboxy-terminal inter-helix linker as the site of phosphatidylinositol 4,5-bisphosphate action on Kv7 (M-type) K+ channels. *J. Gen. Physiol.* 132:361–381. http://dx.doi.org/10.1085/jgp.200810007

Hsu, Y.T., and R.S. Molday. 1993. Modulation of the cGMP-gated channel of rod photoreceptor cells by calmodulin. *Nature.* 361:76–79. http://dx.doi.org/10.1038/361076a0

Huang, C.L., S. Feng, and D.W. Hilgemann. 1998. Direct activation of inward rectifier potassium channels by PIP2 and its stabilization by Gbetagamma. *Nature.* 391:803–806. http://dx.doi.org/10.1038/35882

Huang, Z., R.E. Anderson, W. Cao, A.F. Wiechmann, and R.V.S. Rajala. 2011. Light-induced tyrosine phosphorylation of rod outer segment membrane proteins regulate the translocation, membrane binding and activation of type II α phosphatidylinositol-5-phosphate 4-kinase. *Neurochem. Res.* 36:627–635. http://dx.doi.org/10.1007/s11064-010-0146-y

Ivanovic, I., D.T. Allen, R. Dighe, Y.Z. Le, R.E. Anderson, and R.V.S. Rajala. 2011a. Phosphoinositide 3-kinase signaling in retinal rod photoreceptors. *Invest. Ophthalmol. Vis. Sci.* 52:6355–6362. http://dx.doi.org/10.1167/iovs.10-7138

Ivanovic, I., R.E. Anderson, Y.Z. Le, S.J. Fliesler, D.M. Sherry, and R.V.S. Rajala. 2011b. Deletion of the p85alpha regulatory subunit of phosphoinositide 3-kinase in cone photoreceptor cells results in cone photoreceptor degeneration. *Invest. Ophthalmol. Vis. Sci.* 52:3775–3783. http://dx.doi.org/10.1167/iovs.10-7139

Kaupp, U.B., and R. Seifert. 2002. Cyclic nucleotide-gated ion channels. *Physiol. Rev.* 82:769–824.

Kizhatil, K., S.A. Baker, V.Y. Arshavsky, and V. Bennett. 2009. Ankyrin-G promotes cyclic nucleotide-gated channel transport to rod photoreceptor sensory cilia. *Science.* 323:1614–1617. http://dx.doi.org/10.1126/science.1169789

Ko, G.Y.-P., M.L. Ko, and S.E. Dryer. 2003. Circadian phase-dependent modulation of cGMP-gated channels of cone photoreceptors by dopamine and D2 agonist. *J. Neurosci.* 23:3145–3153.

Ko, G.Y.-P., M.L. Ko, and S.E. Dryer. 2004. Circadian regulation of cGMP-gated channels of vertebrate cone photoreceptors: role of cAMP and Ras. *J. Neurosci.* 24:1296–1304. http://dx.doi.org/10.1523/JNEUROSCI.3560-03.2004

Ko, M.L., K. Jian, L. Shi, and G.Y.-P. Ko. 2009. Phosphatidylinositol 3 kinase-Akt signaling serves as a circadian output in the retina. *J. Neurochem.* 108:1607–1620. http://dx.doi.org/10.1111/j.1471-4159.2009.05931.x

Kurahashi, T., and A. Menini. 1997. Mechanism of odorant adaptation in the olfactory receptor cell. *Nature.* 385:725–729. http://dx.doi.org/10.1038/385725a0

Kusch, J., T. Zimmer, J. Holschuh, C. Biskup, E. Schulz, V. Nache, and K. Benndorf. 2010. Role of the S4-S5 linker in CNG channel activation. *Biophys. J.* 99:2488–2496. http://dx.doi.org/10.1016/j.bpj.2010.07.041

Li, G., A. Rajala, A.F. Wiechmann, R.E. Anderson, and R.V.S. Rajala. 2008. Activation and membrane binding of retinal protein kinase Balpha/Akt1 is regulated through light-dependent generation of

phosphoinositides. *J. Neurochem.* 107:1382–1397. http://dx.doi.org/10.1111/j.1471-4159.2008.05707.x

Liu, C., and M.D. Varnum. 2005. Functional consequences of progressive cone dystrophy-associated mutations in the human cone photoreceptor cyclic nucleotide-gated channel CNGA3 subunit. *Am. J. Physiol. Cell Physiol.* 289:C187–C198. http://dx.doi.org/10.1152/ajpcell.00490.2004

Liu, M., T.Y. Chen, B. Ahamed, J. Li, and K.W. Yau. 1994. Calcium-calmodulin modulation of the olfactory cyclic nucleotide-gated cation channel. *Science.* 266:1348–1354. http://dx.doi.org/10.1126/science.266.5189.1348

Matulef, K., and W.N. Zagotta. 2002. Multimerization of the ligand binding domains of cyclic nucleotide-gated channels. *Neuron.* 36:93–103. http://dx.doi.org/10.1016/S0896-6273(02)00878-4

Matulef, K., G.E. Flynn, and W.N. Zagotta. 1999. Molecular rearrangements in the ligand-binding domain of cyclic nucleotide-gated channels. *Neuron.* 24:443–452. http://dx.doi.org/10.1016/S0896-6273(00)80857-0

Michailidis, I.E., T.D. Helton, V.I. Petrou, T. Mirshahi, M.D. Ehlers, and D.E. Logothetis. 2007. Phosphatidylinositol-4,5-bisphosphate regulates NMDA receptor activity through alpha-actinin. *J. Neurosci.* 27:5523–5532. http://dx.doi.org/10.1523/JNEUROSCI.4378-06.2007

Michalakis, S., X. Zong, E. Becirovic, V. Hammelmann, T. Wein, K.T. Wanner, and M. Biel. 2011. The glutamic acid-rich protein is a gating inhibitor of cyclic nucleotide-gated channels. *J. Neurosci.* 31:133–141. http://dx.doi.org/10.1523/JNEUROSCI.4735-10.2011

Molokanova, E., F. Maddox, C.W. Luetje, and R.H. Kramer. 1999. Activity-dependent modulation of rod photoreceptor cyclic nucleotide-gated channels mediated by phosphorylation of a specific tyrosine residue. *J. Neurosci.* 19:4786–4795.

Möttig, H., J. Kusch, T. Zimmer, A. Scholle, and K. Benndorf. 2001. Molecular regions controlling the activity of CNG channels. *J. Gen. Physiol.* 118:183–192. http://dx.doi.org/10.1085/jgp.118.2.183

Muskett, F.W., S. Thouta, S.J. Thomson, A. Bowen, P.J. Stansfeld, and J.S. Mitcheson. 2011. Mechanistic insight into human ether-à-go-go-related gene (hERG) K+ channel deactivation gating from the solution structure of the EAG domain. *J. Biol. Chem.* 286:6184–6191. http://dx.doi.org/10.1074/jbc.M110.199364

Otsuguro, K., J. Tang, Y. Tang, R. Xiao, M. Freichel, V. Tsvilovskyy, S. Ito, V. Flockerzi, M.X. Zhu, and A.V. Zholos. 2008. Isoform-specific inhibition of TRPC4 channel by phosphatidylinositol 4,5-bisphosphate. *J. Biol. Chem.* 283:10026–10036. http://dx.doi.org/10.1074/jbc.M707306200

Peng, C., E.D. Rich, C.A. Thor, and M.D. Varnum. 2003a. Functionally important calmodulin-binding sites in both NH2- and COOH-terminal regions of the cone photoreceptor cyclic nucleotide-gated channel CNGB3 subunit. *J. Biol. Chem.* 278:24617–24623. http://dx.doi.org/10.1074/jbc.M301699200

Peng, C., E.D. Rich, and M.D. Varnum. 2003b. Achromatopsia-associated mutation in the human cone photoreceptor cyclic nucleotide-gated channel CNGB3 subunit alters the ligand sensitivity and pore properties of heteromeric channels. *J. Biol. Chem.* 278:34533–34540. http://dx.doi.org/10.1074/jbc.M305102200

Peng, C., E.D. Rich, and M.D. Varnum. 2004. Subunit configuration of heteromeric cone cyclic nucleotide-gated channels. *Neuron.* 42:401–410. http://dx.doi.org/10.1016/S0896-6273(04)00225-9

Pugh, E.N. Jr., S. Nikonov, and T.D. Lamb. 1999. Molecular mechanisms of vertebrate photoreceptor light adaptation. *Curr. Opin. Neurobiol.* 9:410–418. http://dx.doi.org/10.1016/S0959-4388(99)80062-2

Rajala, R.V., and R.E. Anderson. 2001. Interaction of the insulin receptor beta-subunit with phosphatidylinositol 3-kinase in bovine ROS. *Invest. Ophthalmol. Vis. Sci.* 42:3110–3117.

Rajala, R.V.S., M.D. Chan, and A. Rajala. 2005. Lipid-protein interactions of growth factor receptor-bound protein 14 in insulin receptor signaling. *Biochemistry.* 44:15461–15471. http://dx.doi.org/10.1021/bi0513148

Rebrik, T.I., and J.I. Korenbrot. 2004. In intact mammalian photoreceptors, Ca2+-dependent modulation of cGMP-gated ion channels is detectable in cones but not in rods. *J. Gen. Physiol.* 123:63–75. http://dx.doi.org/10.1085/jgp.200308952

Rebrik, T.I., I. Botchkina, V.Y. Arshavsky, C.M. Craft, and J.I. Korenbrot. 2012. CNG-modulin: a novel Ca-dependent modulator of ligand sensitivity in cone photoreceptor cGMP-gated ion channels. *J. Neurosci.* 32:3142–3153. http://dx.doi.org/10.1523/JNEUROSCI.5518-11.2012

Rodriguez-Menchaca, A.A., S.K. Adney, Q.-Y. Tang, X.-Y. Meng, A. Rosenhouse-Dantsker, M. Cui, and D.E. Logothetis. 2012. PIP2 controls voltage-sensor movement and pore opening of Kv channels through the S4-S5 linker. *Proc. Natl. Acad. Sci. USA.* 109:E2399–E2408. http://dx.doi.org/10.1073/pnas.1207901109

Rosenbaum, T., and S.E. Gordon. 2002. Dissecting intersubunit contacts in cyclic nucleotide-gated ion channels. *Neuron.* 33:703–713. http://dx.doi.org/10.1016/S0896-6273(02)00599-8

Rosenhouse-Dantsker, A., and D.E. Logothetis. 2007. Molecular characteristics of phosphoinositide binding. *Pflugers Arch.* 455:45–53. http://dx.doi.org/10.1007/s00424-007-0291-6

Sagoo, M.S., and L. Lagnado. 1996. The action of cytoplasmic calcium on the cGMP-activated channel in salamander rod photoreceptors. *J. Physiol.* 497:309–319.

Shuart, N.G., Y. Haitin, S.S. Camp, K.D. Black, and W.N. Zagotta. 2011. Molecular mechanism for 3:1 subunit stoichiometry of rod cyclic nucleotide-gated ion channels. *Nat Commun.* 2:457. http://dx.doi.org/10.1038/ncomms1466

Spehr, M., C.H. Wetzel, H. Hatt, and B.W. Ache. 2002. 3-phosphoinositides modulate cyclic nucleotide signaling in olfactory receptor neurons. *Neuron.* 33:731–739. http://dx.doi.org/10.1016/S0896-6273(02)00610-4

Suh, B.-C., and B. Hille. 2008. PIP2 is a necessary cofactor for ion channel function: how and why? *Annu Rev Biophys.* 37:175–195. http://dx.doi.org/10.1146/annurev.biophys.37.032807.125859

Sunderman, E.R., and W.N. Zagotta. 1999. Sequence of events underlying the allosteric transition of rod cyclic nucleotide-gated channels. *J. Gen. Physiol.* 113:621–640. http://dx.doi.org/10.1085/jgp.113.5.621

Taraska, J.W., M.C. Puljung, N.B. Olivier, G.E. Flynn, and W.N. Zagotta. 2009. Mapping the structure and conformational movements of proteins with transition metal ion FRET. *Nat. Methods.* 6:532–537. http://dx.doi.org/10.1038/nmeth.1341

Trudeau, M.C., and W.N. Zagotta. 2002. An intersubunit interaction regulates trafficking of rod cyclic nucleotide-gated channels and is disrupted in an inherited form of blindness. *Neuron.* 34:197–207. http://dx.doi.org/10.1016/S0896-6273(02)00647-5

Trudeau, M.C., and W.N. Zagotta. 2003. Calcium/calmodulin modulation of olfactory and rod cyclic nucleotide-gated ion channels. *J. Biol. Chem.* 278:18705–18708. http://dx.doi.org/10.1074/jbc.R300001200

Ukhanov, K., D. Brunert, E.A. Corey, and B.W. Ache. 2011. Phosphoinositide 3-kinase-dependent antagonism in mammalian olfactory receptor neurons. *J. Neurosci.* 31:273–280. http://dx.doi.org/10.1523/JNEUROSCI.3698-10.2011

Varnum, M.D., and W.N. Zagotta. 1997. Interdomain interactions underlying activation of cyclic nucleotide-gated channels. *Science.* 278:110–113. http://dx.doi.org/10.1126/science.278.5335.110

Varnum, M.D., K.D. Black, and W.N. Zagotta. 1995. Molecular mechanism for ligand discrimination of cyclic nucleotide-gated channels. *Neuron.* 15:619–625. http://dx.doi.org/10.1016/0896-6273(95)90150-7

Weitz, D., N. Ficek, E. Kremmer, P.J. Bauer, and U.B. Kaupp. 2002. Subunit stoichiometry of the CNG channel of rod photoreceptors. *Neuron.* 36:881–889. http://dx.doi.org/10.1016/S0896-6273(02)01098-X

Winks, J.S., S. Hughes, A.K. Filippov, L. Tatulian, F.C. Abogadie, D.A. Brown, and S.J. Marsh. 2005. Relationship between membrane phosphatidylinositol-4,5-bisphosphate and receptor-mediated inhibition of native neuronal M channels. *J. Neurosci.* 25:3400–3413. http://dx.doi.org/10.1523/JNEUROSCI.3231-04.2005

Womack, K.B., S.E. Gordon, F. He, T.G. Wensel, C.C. Lu, and D.W. Hilgemann. 2000. Do phosphatidylinositides modulate vertebrate phototransduction? *J. Neurosci.* 20:2792–2799.

Young, E.C., and N. Krougliak. 2004. Distinct structural determinants of efficacy and sensitivity in the ligand-binding domain of cyclic nucleotide-gated channels. *J. Biol. Chem.* 279:3553–3562. http://dx.doi.org/10.1074/jbc.M310545200

Zagotta, W.N., N.B. Olivier, K.D. Black, E.C. Young, R. Olson, and E. Gouaux. 2003. Structural basis for modulation and agonist specificity of HCN pacemaker channels. *Nature.* 425:200–205. http://dx.doi.org/10.1038/nature01922

Zhainazarov, A.B., M. Spehr, C.H. Wetzel, H. Hatt, and B.W. Ache. 2004. Modulation of the olfactory CNG channel by Ptdlns(3,4,5)P3. *J. Membr. Biol.* 201:51–57. http://dx.doi.org/10.1007/s00232-004-0707-4

Zhao, X., P. Várnai, G. Tuymetova, A. Balla, Z.E. Tóth, C. Oker-Blom, J. Roder, A. Jeromin, and T. Balla. 2001. Interaction of neuronal calcium sensor-1 (NCS-1) with phosphatidylinositol 4-kinase beta stimulates lipid kinase activity and affects membrane trafficking in COS-7 cells. *J. Biol. Chem.* 276:40183–40189.

Zheng, J., and W.N. Zagotta. 2004. Stoichiometry and assembly of olfactory cyclic nucleotide-gated channels. *Neuron.* 42:411–421. http://dx.doi.org/10.1016/S0896-6273(04)00253-3

Zheng, J., M.C. Trudeau, and W.N. Zagotta. 2002. Rod cyclic nucleotide-gated channels have a stoichiometry of three CNGA1 subunits and one CNGB1 subunit. *Neuron.* 36:891–896. http://dx.doi.org/10.1016/S0896-6273(02)01099-1

Zheng, J., M.D. Varnum, and W.N. Zagotta. 2003. Disruption of an intersubunit interaction underlies Ca2+-calmodulin modulation of cyclic nucleotide-gated channels. *J. Neurosci.* 23:8167–8175.

Zheng, Q., J.A. Bobich, J. Vidugiriene, S.C. McFadden, F. Thomas, J. Roder, and A. Jeromin. 2005. Neuronal calcium sensor-1 facilitates neuronal exocytosis through phosphatidylinositol 4-kinase. *J. Neurochem.* 92:442–451. http://dx.doi.org/10.1111/j.1471-4159.2004.02897.x

Zhong, H., L.L. Molday, R.S. Molday, and K.-W. Yau. 2002. The heteromeric cyclic nucleotide-gated channel adopts a 3A:1B stoichiometry. *Nature.* 420:193–198. http://dx.doi.org/10.1038/nature01201

Zhong, H., J. Lai, and K.-W. Yau. 2003. Selective heteromeric assembly of cyclic nucleotide-gated channels. *Proc. Natl. Acad. Sci. USA.* 100:5509–5513. http://dx.doi.org/10.1073/pnas.0931279100

Zhou, L., and S.A. Siegelbaum. 2007. Gating of HCN channels by cyclic nucleotides: residue contacts that underlie ligand binding, selectivity, and efficacy. *Structure.* 15:655–670. http://dx.doi.org/10.1016/j.str.2007.04.012